NACA RM H56G11

NACA

RESEARCH MEMORANDUM

FLIGHT EVALUATION OF THE LATERAL STABILITY AND CONTROL CHARACTERISTICS OF THE CONVAIR YF-102 AIRPLANE

By Thomas R. Sisk, William H. Andrews,
and Robert W. Darville

High-Speed Flight Station
Edwards, Calif.

NATIONAL ADVISORY COMMITTEE
FOR AERONAUTICS

WASHINGTON

January 16, 1957
Declassified December 8, 1961

NATIONAL ADVISORY COMMITTEE FOR AERONAUTICS

RESEARCH MEMORANDUM

FLIGHT EVALUATION OF THE LATERAL STABILITY AND CONTROL CHARACTERISTICS OF THE CONVAIR YF-102 AIRPLANE

By Thomas R. Sisk, William H. Andrews,
and Robert W. Darville

SUMMARY

The lateral stability and control characteristics were investigated on the Convair YF-102 airplane during flights of the National Advisory Committee for Aeronautics research program. The investigation included gradually increasing sideslips, rudder-fixed aileron rolls, rudder pulses, and trim runs at altitudes of 25,000 and 40,000 feet over the test Mach number range. A few wind-up turns were performed at an altitude of 50,000 feet to investigate directional stability at high lifts.

The lateral handling characteristics appeared satisfactory when viewed in terms of gradually increasing sideslips. A large directional trim change was encountered at all altitudes at a Mach number of approximately 0.95 and a directional divergence was encountered at high lifts (angle of attack approximately 20°). The lateral dynamic stability characteristics were generally unsatisfactory but more tolerable at the higher speeds. Violent inertial coupling was encountered during aileron rolls at a Mach number of 0.74; however, no difficulty was encountered when observing the restriction of rate of roll of 100° per second and angle of bank of 100°.

INTRODUCTION

The YF-102 airplane was designed as a high-performance, all-weather interceptor, and is currently undergoing flight evaluation of handling qualities at the NACA High-Speed Flight Station at Edwards, Calif.

The first portion of the flight program was carried out with the original symmetrical wing configuration; however, to improve the drag characteristics of the airplane, the wing leading edge was cambered and the wing trailing edge (outboard of the elevons) was reflexed up 10°.

Only a small amount of lateral stability and control data was obtained with the symmetrical wing configuration; therefore, only the cambered-reflexed wing configuration data are shown in this paper. These tests were carried out at altitudes ranging from 20,000 to 50,000 feet over the Mach number range from 0.44 to 1.17. Violent inertial coupling encountered during this investigation is reported in reference 1.

The flights included in this investigation were performed from November 1954 to October 1955.

SYMBOLS

a_n normal acceleration factor, g units

a_t transverse acceleration factor, g units

b wing span, ft

C_l rolling-moment coefficient, $\frac{\text{Rolling moment}}{\frac{1}{2}\rho V^2 Sb}$

C_{N_A} airplane normal-force coefficient, $\frac{Wa_n}{\frac{1}{2}\rho V^2 S}$

C_n yawing-moment coefficient, $\frac{\text{Yawing moment}}{\frac{1}{2}\rho V^2 Sb}$

C_Y lateral-force coefficient, $\frac{\text{Lateral force}}{\frac{1}{2}\rho V^2 S}$

$\frac{1}{C_{1/2}}$ reciprocal of cycles to damp to one-half amplitude

$\bar{c}$ mean aerodynamic chord, ft

F_a lateral stick force, lb

F_e longitudinal stick force, lb

F_r rudder force, lb

g acceleration due to gravity, ft/sec^2

h_p pressure altitude, ft

I_X	moment of inertia about longitudinal body axis, slug-ft^2
I_{X_e}	moment of inertia of rotating engine parts about X-body axis, slug-ft^2
I_Y	moment of inertia about lateral body axis, slug-ft^2
I_Z	moment of inertia about normal body axis, slug-ft^2
I_{XZ}	product of inertia referred to X- and Z-axis, slug-ft^2
M	Mach number
P	period, sec
p	rolling angular velocity, radians/sec
$\dot{p}$	rolling angular acceleration, radians/sec^2
$\bar{p}$	average rolling velocity, radians/sec
q	pitching angular velocity, radians/sec
$\dot{q}$	pitching angular acceleration, radians/sec^2
r	yawing angular velocity, radians/sec
$\dot{r}$	yawing angular acceleration, radians/sec^2
S	wing area, ft^2
$T_{1/2}$	time to damp to one-half amplitude, sec
t	time, sec
$t_{\varphi=90^\circ}$	time to bank to 90°, sec
V	true velocity, ft/sec
V_e	equivalent velocity, $V\sqrt{\sigma}$, ft/sec
V_i	indicated velocity, mph
v_e	equivalent side velocity, $\frac{\beta V_e}{57.3}$, ft/sec

W airplane weight, lb

$\frac{pb}{2V}$ wing-tip helix angle, radians

$\frac{pb/2V}{\delta_a}$ variation of wing-tip helix angle with lateral control angle, per deg

$\frac{da_t}{d\beta}$ variation of transverse acceleration factor with angle of sideslip, g/deg

$\frac{dF_a}{d\beta}$ variation of lateral stick force with angle of sideslip, lb/deg

$\frac{dF_r}{d\beta}$ variation of rudder force with angle of sideslip, lb/deg

$\frac{d\delta_a}{d\beta}$ variation of lateral control angle with angle of sideslip

$\frac{d\delta_r}{d\beta}$ variation of rudder control angle with angle of sideslip

$\frac{dC_l}{d\delta_a}$ variation of rolling-moment coefficient with aileron deflection, per radian

$\frac{dC_l}{d\delta_r}$ variation of rolling-moment coefficient with rudder deflection, per radian

$\frac{dC_n}{d\delta_a}$ variation of yawing-moment coefficient with aileron deflection, per radian

$\frac{dC_n}{d\delta_r}$ variation of yawing-moment coefficient with rudder deflection, per radian

C_{l_β} variation of rolling-moment coefficient with angle of sideslip, $\frac{dC_l}{d\beta}$, per radian

C_{n_β} variation of yawing-moment coefficient with angle of sideslip, $\frac{dC_n}{d\beta}$, per radian

C_{Y_β} variation of lateral-force coefficient with angle of sideslip, $\frac{dC_Y}{d\beta}$, per radian

α angle of attack, deg

β angle of sideslip, deg

δ_a lateral control angle, $\delta_{e_L} - \delta_{e_R}$, right roll positive, deg

δ_e longitudinal control angle, $\frac{\delta_{e_L} + \delta_{e_R}}{2}$, deg

δ_r rudder control angle, deg

δ_{s_a} lateral stick position, in.

δ_{s_e} longitudinal stick position, in.

δ_{p_L} left rudder pedal position, in.

θ angle of pitch relative to flight-path direction, radians

ρ density, slugs/cu ft

σ air density ratio, $\frac{\rho}{\rho_0}$

φ bank angle, deg

ψ angle of yaw relative to flight-path direction, radians

ω_e rotational velocity of engine rotor, radians/sec

$\omega_\theta{}^2$ nondimensional undamped natural frequency in pitch of nonrolling aircraft (ratio of pitching frequency to steady rolling frequency)

$\omega_\psi{}^2$ nondimensional undamped natural frequency in yaw of nonrolling aircraft

Subscripts:

L	left
R	right
0	standard sea-level conditions

AIRPLANE

The test airplane is illustrated by the three-view drawing of figure 1 and the photographs of figure 2. Physical characteristics are presented in table I. The airplane is a semitailless, delta-wing configuration having 60° leading-edge sweepback of the wing and vertical stabilizer. The wing configuration embodies a 6.3 percent conical camber leading edge, 10° reflexed tips, and wing fences located at 37 and 67 percent of the wing semispan.

The airplane is equipped with conventional flap-type control surfaces which are actuated by an irreversible hydraulic power control system that is integrated with the stick and rudder pedals through an artificial feel system. The lateral control forces are provided by a simple mechanical spring so that the stick force is a constant function of stick displacement. The rudder forces are provided through a combination of mechanical spring and "q-feel" mechanism.

No pitch or yaw dampers were installed on the airplane during this investigation.

INSTRUMENTATION AND ACCURACY

The airplane was instrumented to record the following quantities pertinent to the stability and control investigation and all instruments were correlated by a common timer:

Airspeed and altitude
Angle of attack and sideslip
Normal and transverse acceleration
Pitch, roll, and yawing velocities and accelerations
Control stick and rudder pedal positions
Elevator, aileron, and rudder positions
Elevator, aileron, and rudder control forces

The airspeed head, angle-of-attack vane, and angle-of-sideslip vane are mounted on a boom extending forward of the fuselage nose. The static pressure and total pressure orifices on the airspeed head are located at points 79 inches and 87 inches, respectively, ahead of the fuselage zero station. The airspeed installation was calibrated by the standard radar phototheodolite method and the Mach number is estimated to be accurate to ±0.01. The angle-of-attack and angle-of-sideslip vanes are located approximately 64 inches forward of the fuselage zero station. The indicated angle-of-attack reading was corrected for errors introduced by boom bending and pitching velocity, but no attempt was made to correct the errors resulting from vane floating or upwash. Corrections to the measured sideslip angles for errors resulting from rolling and yawing velocities are small and have been disregarded.

The airplane weight was determined from the pilot's reading of the fuel quantity gage at the beginning of each maneuver and is estimated to be accurate to ±100 pounds.

TESTS

Gradually increasing sideslips, rudder-fixed aileron rolls, rudder pulses, and trim runs were performed at 25,000 and 40,000 feet over the test Mach number range. During the initial roll investigation, violent inertial coupling was encountered, as reported in reference 1, and subsequent rolling maneuvers were restricted to a rate of roll of 100° per second and an angle of bank of 100°. A few wind-up turns were performed at an altitude of 50,000 feet to investigate the directional divergence predicted by tunnel tests at the higher angles of attack. It was necessary to go to the higher altitude to develop the higher lift coefficient without exceeding the normal acceleration limitation of 3.7g.

Only cambered-reflexed configuration data are presented in this paper since most of the information was obtained with this configuration.

The center of gravity for these tests varied between 28.2 and 29.0 percent of the mean aerodynamic chord.

RESULTS AND DISCUSSION

Static Stability Characteristics

Sideslip characteristics.- A summary of the sideslip characteristics is presented in figures 3 and 4. Figure 3 shows representative basic plots of the variation of longitudinal, lateral, and directional control

angles; transverse acceleration; and lateral and directional force as a function of sideslip angle for three Mach numbers at an altitude of 40,000 feet. Figure 4 summarizes all sideslip data at altitudes of 25,000 and 40,000 feet over the test Mach number range with the XF-92A airplane data (ref. 2) added for comparison. Sideslips on the YF-102 airplane were limited to about 5° but, within this range, the basic plots of figure 3 show the pitching moment resulting from sideslip is small and the variation of rudder control angle and lateral control angle with sideslip is linear. In the summary presentation of figure 4, for comparable altitudes, the variation of transverse acceleration with sideslip $\frac{da_t}{d\beta}$ for the YF-102 airplane is of the order of two-thirds that of the XF-92A airplane. The pilots commented that the sideslip characteristics were satisfactory and that the transverse acceleration was not excessive.

Determination of static derivatives.- Figure 5 presents the variation with Mach number of the static derivatives $C_{l_{\delta_a}}$, $C_{l_{\delta_r}}$, $C_{n_{\delta_a}}$, and $C_{n_{\delta_r}}$ which were used to obtain the effective dihedral parameter C_{l_β} and the directional stability parameter C_{n_β} presented in figure 6. These derivatives and the lateral force parameter C_{Y_β} (fig. 6) were determined according to the method outlined in the appendix for the test altitude of 40,000 feet. The sideslip parameters of figure 6 substantiate the variations of $\frac{d\delta_r}{d\beta}$, $\frac{d\delta_a}{d\beta}$, and $\frac{da_t}{d\beta}$ presented in figure 4.

Directional trim.- The YF-102 airplane experiences a severe directional trim change at all altitudes at a Mach number of about 0.95. Figure 7 presents the rudder trim variation with Mach number at an altitude of 40,000 feet where rudder deflection of 4° and rudder force of 100 pounds is required to maintain a sideslip angle of zero. This abrupt directional trim change is excessive, making precise control of the airplane difficult in this speed range.

Divergence at high lift.- Several wind-up turns were performed with the YF-102 airplane at an altitude of 50,000 feet to study the high lift directional stability characteristics without exceeding the limit load factor of 3.7g. One of these turns to maximum C_{N_A} (fig. 8) exceeded an angle of attack of 20° and the airplane diverged in sideslip to 10° before recovery could be effected. Additional turns have been performed at 50,000 feet to investigate this divergence further; however, buffeting has generally limited these turns to 18° in angle of attack. Two of these turns did exceed 18°, however, and the beginning of a directional divergence was indicated. It would seem, then, that a directional divergence might be anticipated whenever the angle of attack exceeds 20°.

Too few divergences were encountered to obtain reasonably accurate pilot comments on the maneuver; however, with the low pitch rate in the one maneuver where divergence was attained, the pilot felt he could control the divergence by decreasing the angle of attack before extreme values of sideslip were reached.

Dynamic Characteristics

Period and damping.- The period and damping as a function of Mach number and the reciprocal of the cycles to damp to one-half amplitude plotted against $\frac{\varphi}{v_e}$ for comparison with the Specification of reference 3 are presented in figure 9. Inspection of figure 9(a) reveals that P and $T_{1/2}$ vary as might be expected. The Specification states that the damping of the lateral-directional oscillation shall be such that the damping parameter $\frac{1}{C_{1/2}}$ has a value greater than that shown by the curve of figure 9(b). Figure 9(b) shows that the YF-102 in comparison with the Specification varies from unsatisfactory at the low speeds to marginally satisfactory at the high speeds. The pilots felt the lateral period and damping characteristics obtained from rudder pulses were generally unsatisfactory but more tolerable at the higher speeds. This is pointed out in figure 9(b) which shows the pilot's rating of each pulse. The pilots considered the roll-to-yaw (effective dihedral) to be objectionably high over most of the speed range covered in the tests, with the airplane being very sensitive in roll. Also shown in figure 9, for comparison, are XF-92A data for an altitude of 30,000 feet.

Residual oscillations.- Residual oscillations have been encountered at all speeds and altitudes with the YF-102 airplane. These oscillations are not severe enough to restrict the maneuvering capabilities of the airplane, but the pilots felt the oscillation would make the execution of precision maneuvers (tracking runs, for example) extremely difficult. Figure 10 presents time histories of two such runs at low speed at an altitude of approximately 20,000 feet.

Rolling Characteristics

Landing configuration.- Reference 3 states that at low speed the average $\frac{pb}{2V}$ shall equal 0.05 for the first 30° of bank. Figure 11 presents a time history of a low-speed aileron roll with gear down where the average $\frac{pb}{2V}$ equaled 0.036 at a bank angle of 30° showing that the YF-102 airplane will not meet the low-speed roll requirements of the Military Specification. The pilots, however, reported the low-speed rolling characteristics of the YF-102 airplane to be satisfactory.

Clean configuration.- Figure 12(a) presents the variation of wing-tip helix angle with lateral control angle for the higher speeds and shows that this variation is linear over the range of control deflections tested. Figure 12(b) presents the variation of $\frac{pb}{2V}/\delta_a$ with Mach number and the time to bank to 90° for one-quarter and one-half control deflection. Figure 12(b) indicates that the YF-102 airplane, for one-half control deflection, would not meet the Military Specification of $\frac{pb}{2V} = 0.09$ or 1 second to reach an angle of bank of 100°. At higher control deflections, it appears the YF-102 would meet the requirements; however, the airplane is presently limited to 100° per second rate of roll and 100° of bank because of violent inertial coupling that has been encountered.

Roll coupling.- Figure 13(a) is a time history of an aileron roll executed at an altitude of 39,000 feet at $M = 0.74$ in which violent coupling was encountered. The sideslip angle increased to 30° and the normal acceleration exceeded the range of the instrument at -2.6g in this maneuver. After this maneuver, the airplane was restricted to 100° per second rate of roll and 100° angle of bank by the manufacturer. A more complete discussion of this maneuver is found in reference 1. Figure 13(b) presents two representative time histories of restricted rolls at $M = 0.85$ and $M = 1.15$, showing that no excessive amplitudes in angle of attack or sideslip were encountered in observing this limitation. Additional maneuvers were performed observing the roll limitation where the airplane was rolled from wings level to a bank angle of 45°, then from 45° angle of bank in one direction to 45° angle of bank in the opposite direction. The pilots commented that, for these conditions, the lateral control characteristics appeared satisfactory.

Figure 14(a) is a summary of the transonic speed rolls performed at 40,000 feet where the unrestricted rolls that were performed prior to the violent coupling maneuver of figure 13(a) are indicated by solid symbols. This summary plot shows that no appreciable changes in sideslip angle or angle of attack occurred with the restriction of 100° per second rate of roll and 100° angle of bank placed on the airplane, as evidenced by the envelope around the $\Delta\beta$ and $\Delta\alpha$ values. Conversely, the unrestricted rolls show considerably larger changes in $\Delta\beta$ and $\Delta\alpha$, particularly at the lower speeds. The violent maneuver of figure 13(a) is shown in figure 14(a) where the sideslip angle increased to 30° and the angle of attack exceeded a 19° variation from trim. Figure 14(b) presents the low-speed characteristics, gear up and gear down, with the restriction and extends the restricted roll data of figure 14(a) in that no appreciable changes in sideslip angle or angle of attack were encountered. The recovery values of $\Delta\beta$ and $\Delta\alpha$ were generally smaller than the initial values and, for clarity, are omitted from the figure.

Most of the aileron roll data were obtained with the restriction of 100° per second rate of roll and 100° angle of bank in which no violent inertial coupling was anticipated or encountered. There are many factors that influence the severity of roll coupling; however, as pointed out in reference 4, plots of the type presented in figures 15 and 16 can be used as a guide in determining flight conditions where serious roll coupling might be expected in 360° rolls. Figure 15 presents a roll stability plot of the type discussed in reference 4 for the YF-102 airplane at three Mach numbers. It is evident that at all Mach numbers the proportioning of longitudinal to directional stability is such that the initial coupled motion would be primarily a sideslip excursion. Furthermore, this stability proportioning becomes less desirable as Mach number increases. The roll rates at which the lines of figure 15 cross the vertical boundary were shown in reference 4 to correlate fairly well with the average roll rate at which peak coupling effects were obtained in 360° roll calculations. This roll velocity, termed "lower resonant frequency," has been plotted in the flight envelope of figure 16. Also shown in this figure is the approximate maximum average roll rate attainable in 1 g flight. Thus it is seen that roll rates at which serious coupling effects might be obtained are possible throughout most of the test Mach number range for this airplane. As a matter of interest, the flight condition of figure 13(a) is plotted in figure 16. The roll rate of -1.55 radians per second at which peak coupling effects might be expected, correlated rather well with the average roll rate obtained from figure 13(a) (1.57 radians/sec to control reversal).

CONCLUSIONS

Results obtained from the lateral stability and control investigation performed on the YF-102 airplane indicate the following conclusions:

1. The static lateral stability characteristics, as measured in sideslip, appear satisfactory. There is adequate rudder power over the entire speed range.

2. A large directional trim change was encountered at a Mach number of approximately 0.95 at all altitudes.

3. A directional divergence was encountered in wind-up turns where the angle of attack exceeded 20°.

4. The pilots felt that the dynamic characteristics, as measured in rudder pulses, were generally unsatisfactory but more tolerable at the higher speeds.

5. Although the airplane did not meet the Military Specification for the landing configuration, the pilots reported the low-speed rolling characteristics to be satisfactory. Violent inertial coupling was encountered in an aileron roll at a Mach number of 0.74; however, no difficulty was encountered when observing the restriction of rate of roll of 100° per second and angle of bank of 100°.

High-Speed Flight Station,
National Advisory Committee for Aeronautics,
Edwards, Calif., June 25, 1956.

REFERENCES

1. Sisk, Thomas R., and Andrews, William H.: Flight Experience With A Delta-Wing Airplane Having Violent Lateral-Longitudinal Coupling in Aileron Rolls. NACA RM H55H03, 1955.

2. Sisk, Thomas R., and Muhleman, Duane O.: Lateral Stability and Control Characteristics of the Convair XF-92A Delta-Wing Airplane as Measured in Flight. NACA RM H55A17, 1955.

3. Anon.: Military Specification - Flying Qualities of Piloted Airplanes. MIL-F-8785(ASG), 1 September 1954.

4. Weil, Joseph, and Day, Richard E.: An Analog Study of the Relative Importance of Various Factors Affecting Roll Coupling. NACA RM H56A06, 1956.

APPENDIX

The variation of the effective dihedral parameter C_{l_β}, the directional stability parameter C_{n_β}, and the lateral-force parameter C_{Y_β} were determined for the YF-102 airplane from the following equations

$$C_{l_\beta} = -\left[\left(\frac{dC_l}{d\delta_a}\right)\left(\frac{d\delta_a}{d\beta}\right) + \left(\frac{dC_l}{d\delta_r}\right)\left(\frac{d\delta_r}{d\beta}\right)\right] \tag{1}$$

$$C_{n_\beta} = -\left[\left(\frac{dC_n}{d\delta_r}\right)\left(\frac{d\delta_r}{d\beta}\right) + \left(\frac{dC_n}{d\delta_a}\right)\left(\frac{d\delta_a}{d\beta}\right)\right] \tag{2}$$

$$C_{Y_\beta} = \frac{W\left(\frac{|da_t|}{|d\beta|}\right)}{\frac{1}{2}\rho V^2 S} \tag{3}$$

The basic $\dot{r}$ and $\dot{p}$ equations of motion about the body axis are

$$\dot{p} = \left(\frac{I_Y - I_Z}{I_X}\right)qr + \frac{I_{XZ}}{I_X}\dot{r} + \frac{I_{XZ}}{I_X}pq + \frac{ASb}{I_X}C_{l_{\delta_a}}\delta_a + \frac{ASb}{I_X}C_{l_{\delta_r}}\delta_r + \frac{ASb^2}{2VI_X}C_{l_p}p + \frac{ASb^2}{2VI_X}C_{l_r}r + \frac{ASb}{I_X}C_{l_\beta}\beta + \frac{ASb^2}{2VI_X}C_{l_{\dot{\beta}}}\dot{\beta} \tag{4}$$

$$\dot{r} = \left(\frac{I_X - I_Y}{I_Z}\right)pq + \frac{I_{XZ}}{I_Z}\dot{p} - \frac{I_{XZ}}{I_Z}qr + \frac{I_{X_e}\omega_e}{I_Z}q + \frac{ASb}{I_Z}C_{n_{\delta_r}}\delta_r + \frac{ASb^2}{2VI_Z}C_{n_r}r + \frac{ASb^2}{2VI_Z}C_{n_p}p + \frac{ASb}{I_Z}C_{n_\beta}\beta + \frac{ASb^2}{2VI_Z}C_{n_{\dot{\beta}}}\dot{\beta} + \frac{ASb}{I_Z}C_{n_{\delta_a}}\delta_a \tag{5}$$

where

$$A = \frac{1}{2}\rho V^2$$

If the accelerations are considered before the angular velocities and displacements reach appreciable values, and if the other second order effects are neglected, equations (4) and (5) reduce to

$$\dot{p} = \frac{ASb}{I_X} C_{l_{\delta_a}} \delta_a + \frac{ASb}{I_X} C_{l_{\delta_r}} \delta_r \tag{6}$$

$$\dot{r} = \frac{ASb}{I_Z} C_{n_{\delta_r}} \delta_r + \frac{ASb}{I_Z} C_{n_{\delta_a}} \delta_a + \frac{I_{XZ}}{I_Z} \dot{p} \tag{7}$$

The variation of rolling- and yawing-moment coefficient with respect to aileron and rudder deflection was determined by using equations (6) and (7) from the initial phase of rudder pulses and rudder-fixed aileron rolls as follows

$$\frac{dC_l}{d\delta_a} = \frac{I_X \Delta\dot{p}}{\frac{1}{2}\rho V^2 Sb} \Big/ \Delta\delta_a \quad \text{from rudder-fixed aileron rolls} \tag{8}$$

$$\frac{dC_l}{d\delta_r} = \frac{I_X \Delta\dot{p}}{\frac{1}{2}\rho V^2 Sb} \Big/ \Delta\delta_r \quad \text{from rudder pulses} \tag{9}$$

$$\frac{dC_n}{d\delta_r} = \frac{I_Z \Delta\dot{r}}{\frac{1}{2}\rho V^2 Sb} \Big/ \Delta\delta_r \quad \text{from rudder pulses} \tag{10}$$

$$\frac{dC_n}{d\delta_a} = \frac{I_Z}{ASb\Delta\delta_a} \left[\Delta\dot{r} - \frac{I_{XZ}}{I_Z} \Delta\dot{p}\right] \quad \text{from rudder-fixed aileron rolls} \tag{11}$$

The following plots show representative magnitudes of $\dot{r}$ and $\dot{p}$ and times considered in analyzing the rudder-fixed aileron rolls and rudder pulses.

In determining C_{Y_β}, the control-fixed portion of the rudder pulses was used to determine the variation of transverse acceleration with sideslip angle.

Typical Rudder-Fixed Aileron Roll and Rudder Pulse Used in Determining $C_{l_{\delta_a}}$, $C_{l_{\delta_r}}$, $C_{n_{\delta_a}}$, and $C_{n_{\delta_r}}$

h_p = 40,000 feet

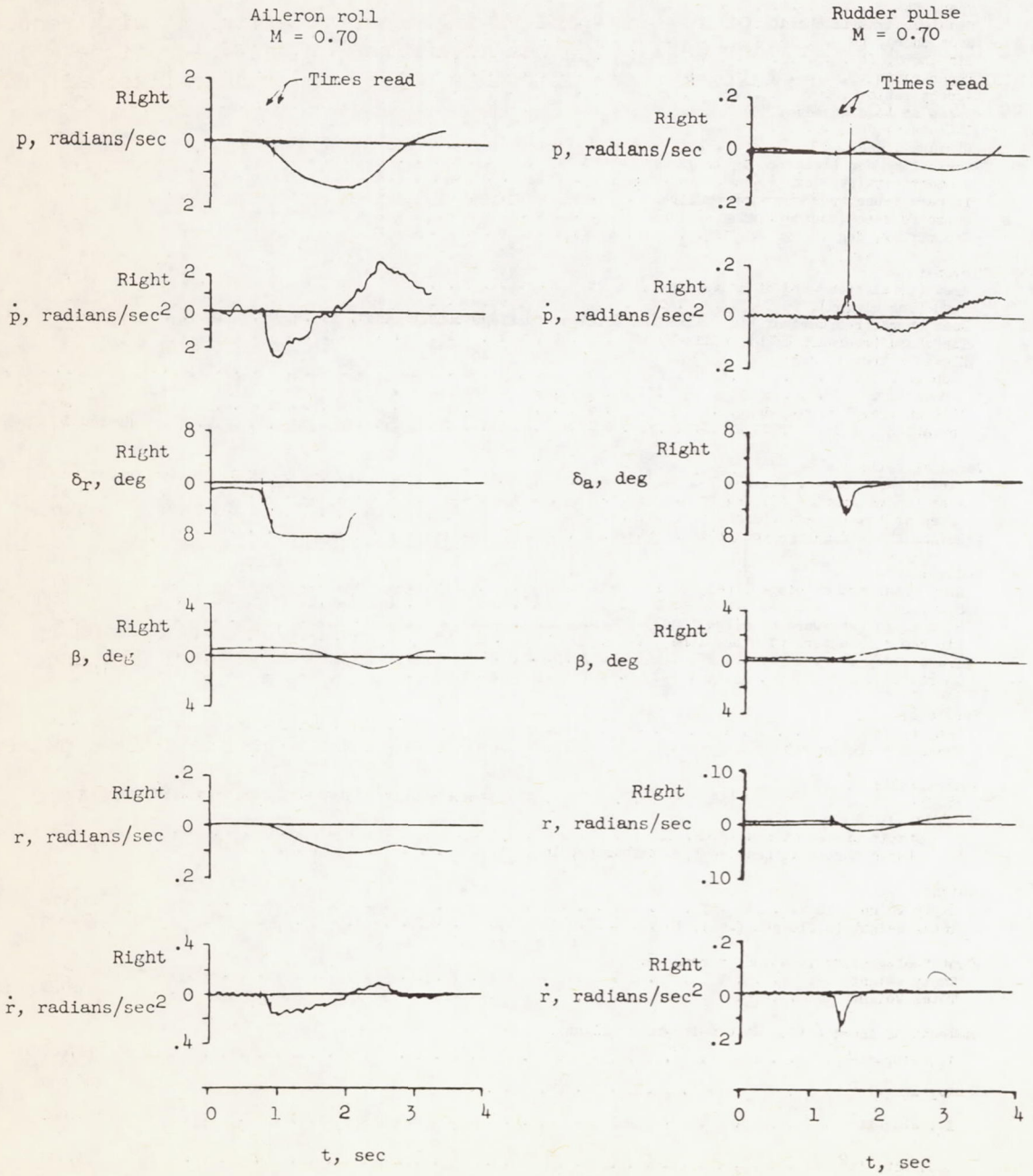

TABLE I

PHYSICAL CHARACTERISTICS OF THE TEST AIRPLANE

Wing:	
Airfoil section	NACA 0004-65 (modified)
Total area, sq ft	695.05
Span, ft	38.19
Mean aerodynamic chord, ft	23.75
Root chord, ft	35.63
Tip chord, ft	0.81
Taper ratio	0.023
Aspect ratio	2.08
Sweep at leading edge, deg	60°6'
Incidence, deg	0
Dihedral, deg	0
Conical camber (leading edge), percent chord	6.3
Geometric twist, deg	0
Inboard fence, percent wing semispan	37
Outboard fence, percent wing semispan	67
Tip reflex, deg	10
Elevons:	
Area (total, rearward of hinge line), sq ft	67.77
Span (one elevon), ft	13.26
Root chord (rearward of hinge line, parallel to fuselage center line), ft	3.15
Tip chord (rearward of hinge line), ft	2.03
Elevator travel, deg:	
Up	35
Down	20
Aileron travel total, deg	20
Operation	Hydraulic
Vertical tail:	
Airfoil section	NACA 0004-65 (modified)
Area (above station 33), sq ft	68.33
Sweep at leading edge, deg	60
Height above fuselage center line, ft	11.41
Rudder:	
Area (rearward of hinge line), sq ft	10.47
Span, ft	5.63
Root chord (rearward of hinge line), ft	2.10
Tip chord (rearward of hinge line), ft	1.61
Travel, deg	±25
Operation	Hydraulic
Fuselage:	
Length, ft	52.4
Maximum diameter, ft	6.5
Power plant:	
Engine	Pratt & Whitney J57-P-11 turbojet with afterburner
Rating:	
Static thrust at sea level, lb	9,700
Static thrust at sea level, afterburner, lb	14,800
Weight:	
Empty weight, lb	21,235
Total weight (1,010 gal fuel), lb	27,800
Center-of-gravity location, percent $\bar{c}$:	
Empty weight	25.6
Total weight	29.8
Moments of inertia (for 24,000-lb gross weight):	
I_X, slug-ft^2	13,200
I_Y, slug-ft^2	106,000
I_Z, slug-ft^2	114,600
I_{XZ}, slug-ft^2	3,540
Inclination of principal axis below reference axis at nose, deg	2

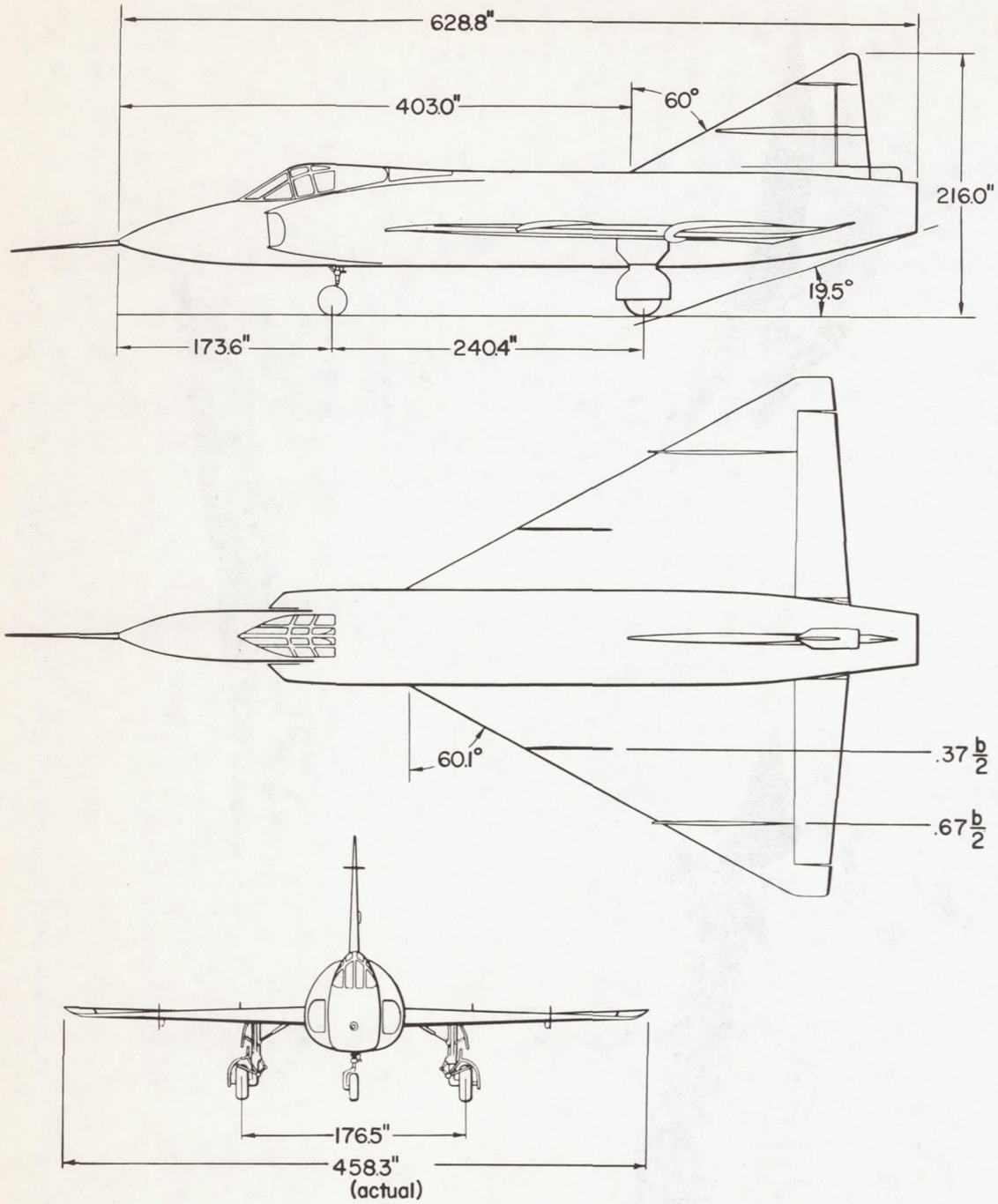

Figure 1.- Three-view drawing of YF-102 airplane.

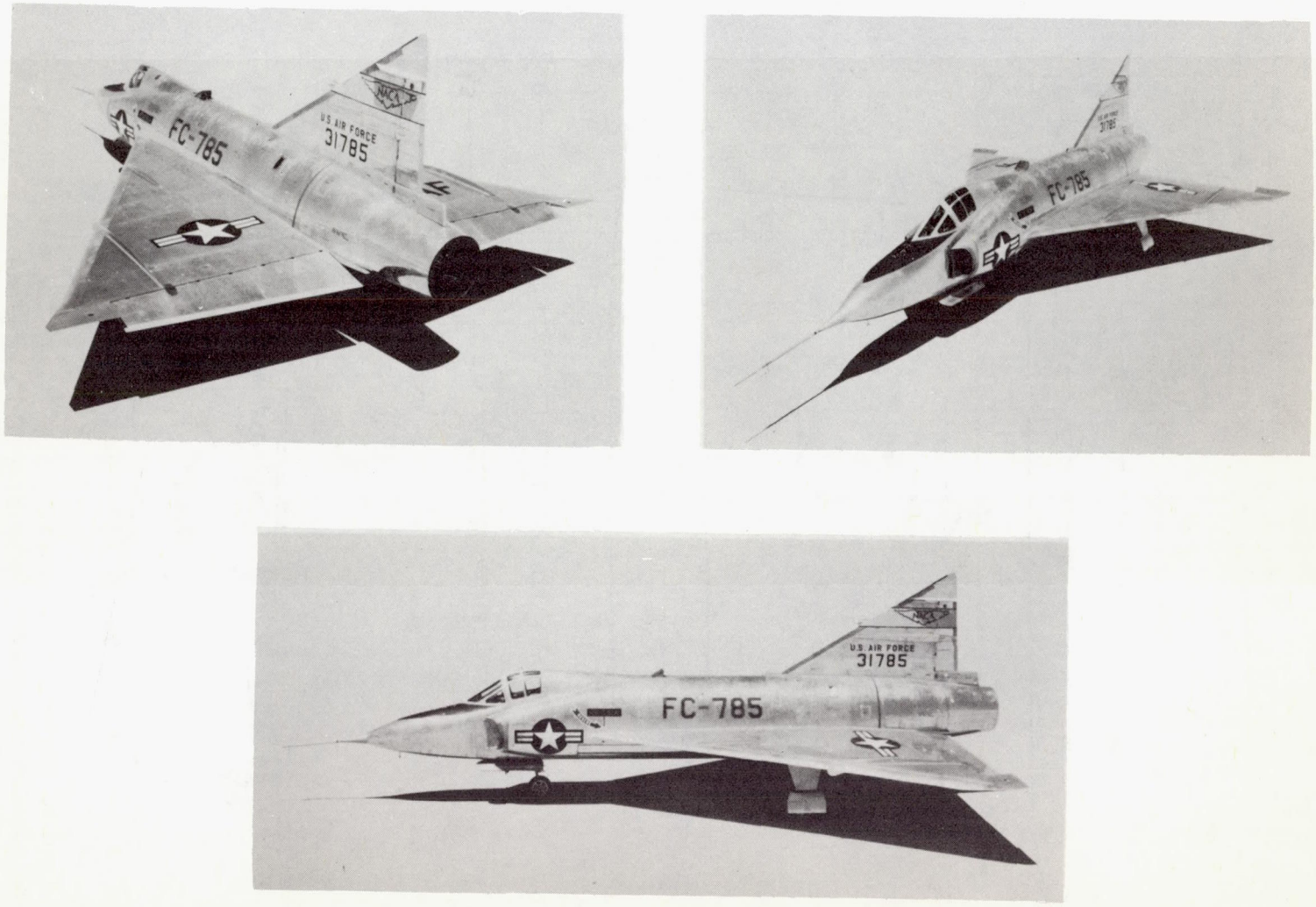

Figure 2.- Photographs of the YF-102 airplane with cambered wing.

L-93572

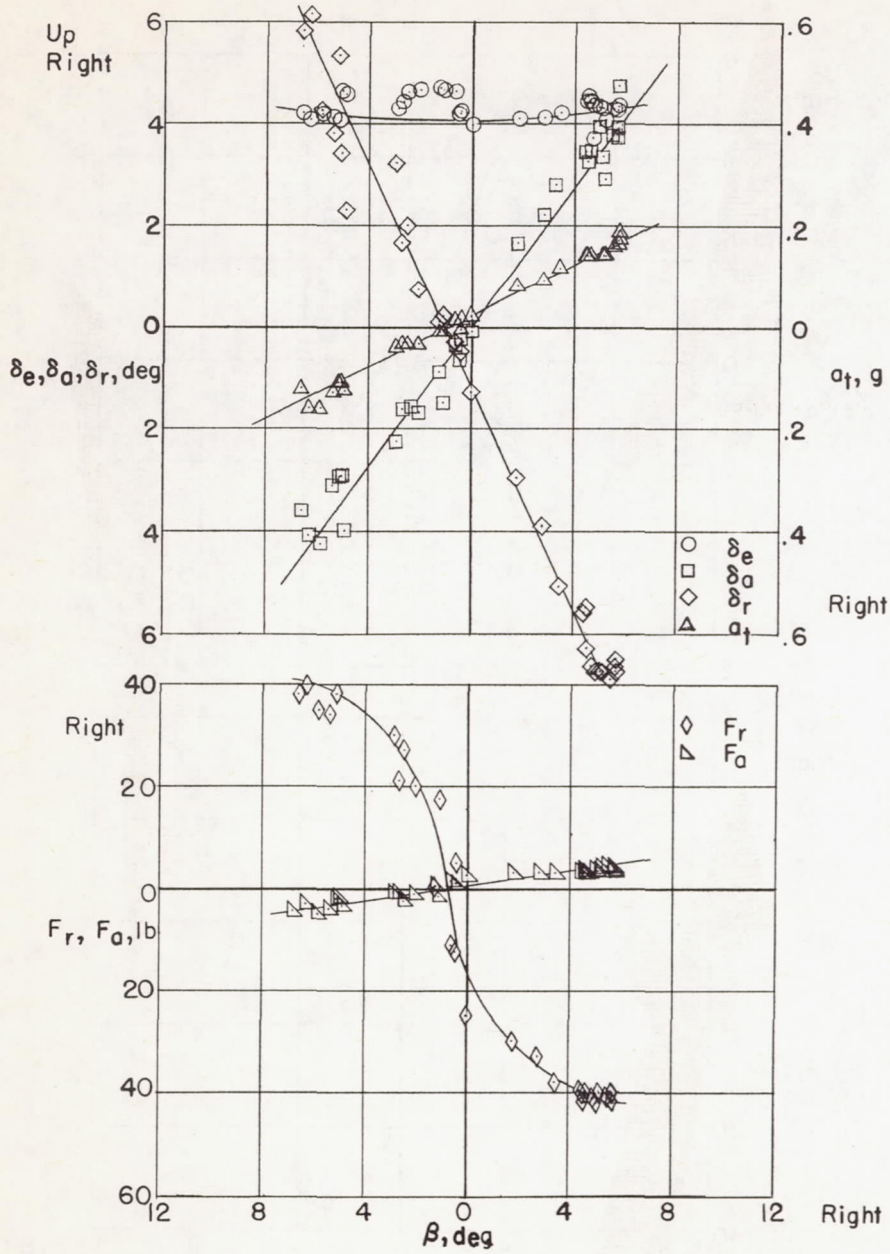

(a) $M = 0.71$; $h_p = 40{,}100$ feet; $C_{N_A} = 0.265$; $\alpha = 8.4^{\circ}$.

Figure 3.- Typical variations of control positions, transverse acceleration, and aileron and rudder force with sideslip angle. YF-102 airplane.

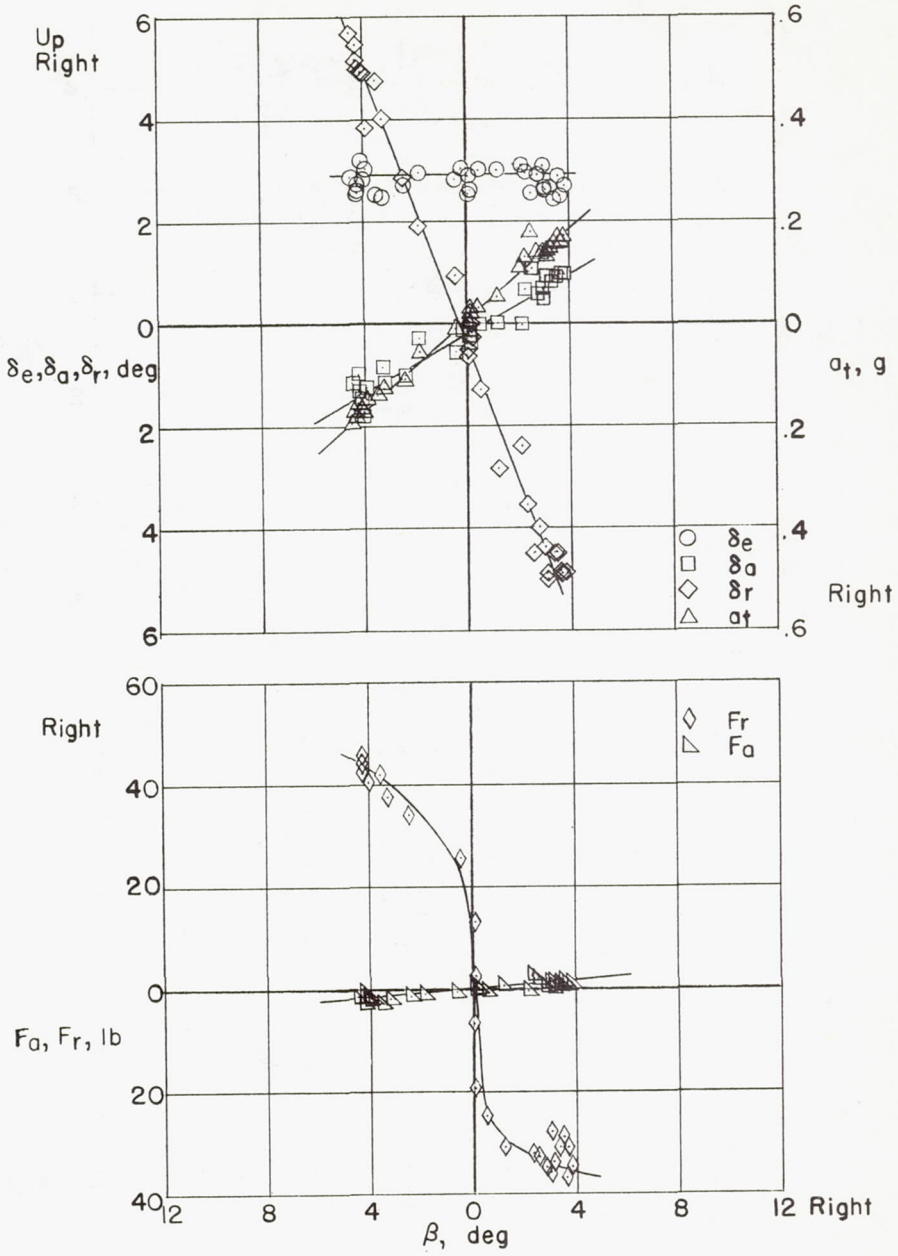

(b) $M = 0.90$; $h_p = 40{,}500$ feet; $C_{N_A} = 0.167$; $\alpha = 5.0^{\circ}$.

Figure 3.- Continued.

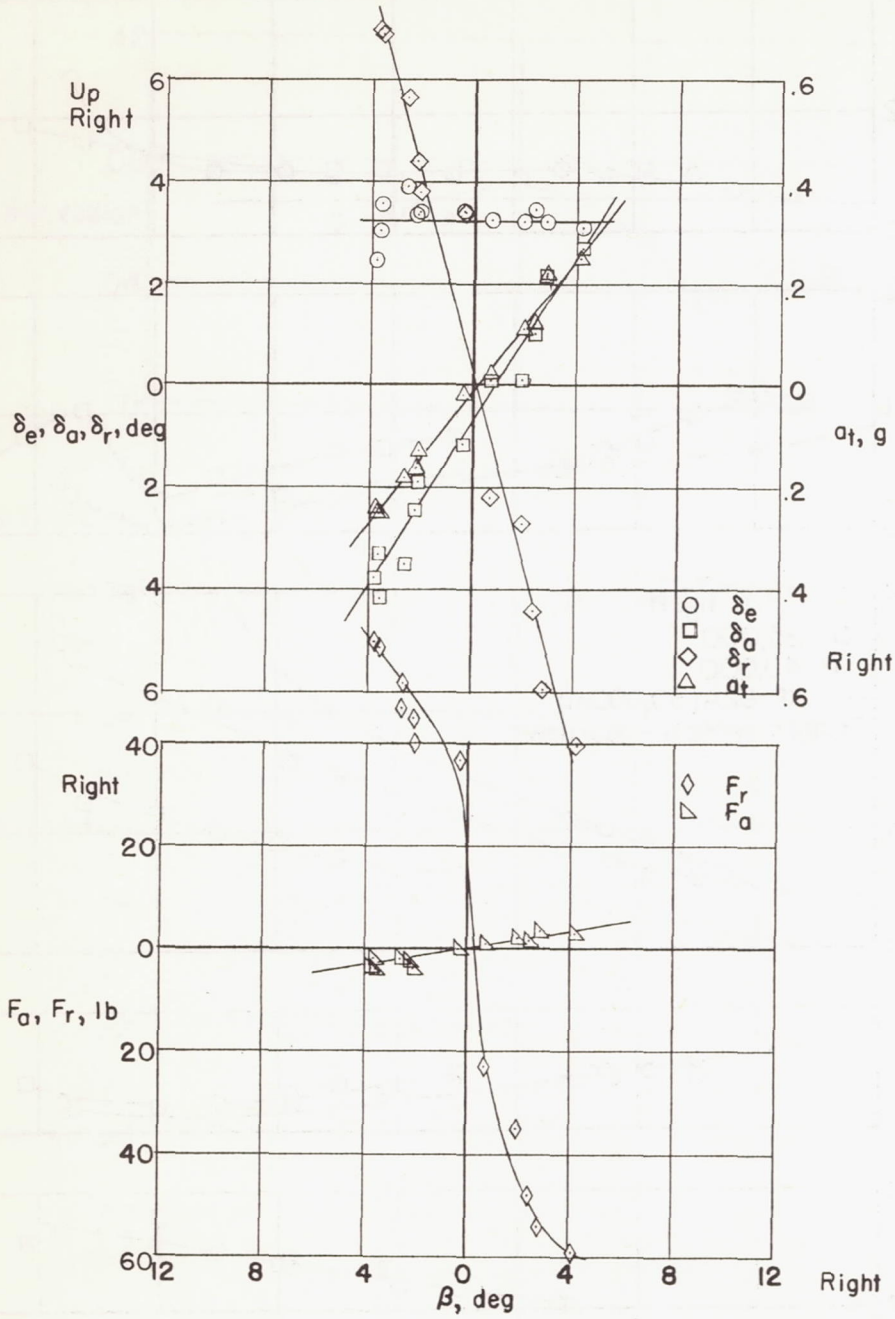

(c) $M = 1.01$; $h_p = 40{,}520$ feet; $C_{N_A} = 0.132$; $\alpha = 4.0^\circ$.

Figure 3.- Concluded.

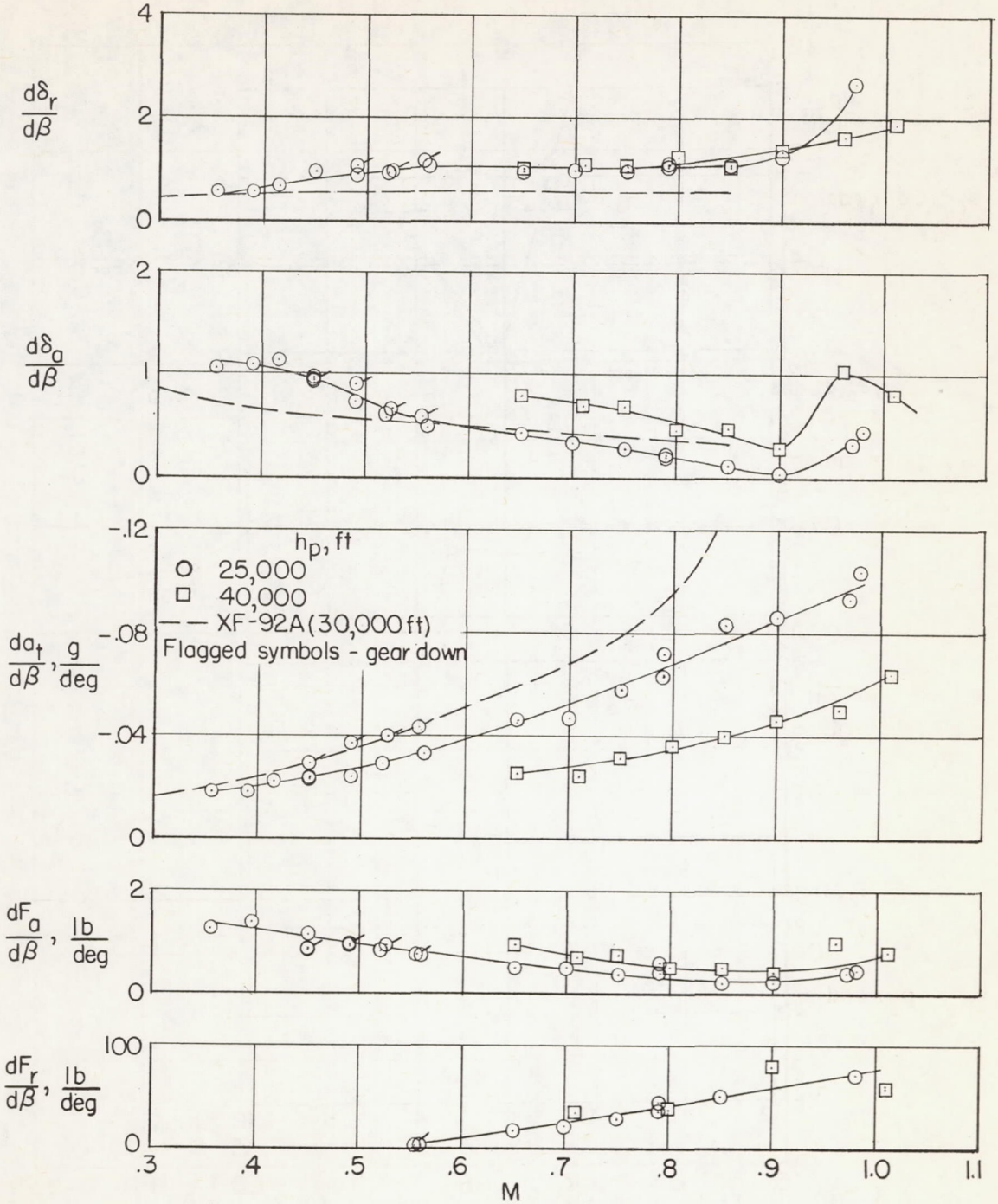

Figure 4.- Summary of the sideslip characteristics of the YF-102 airplane.

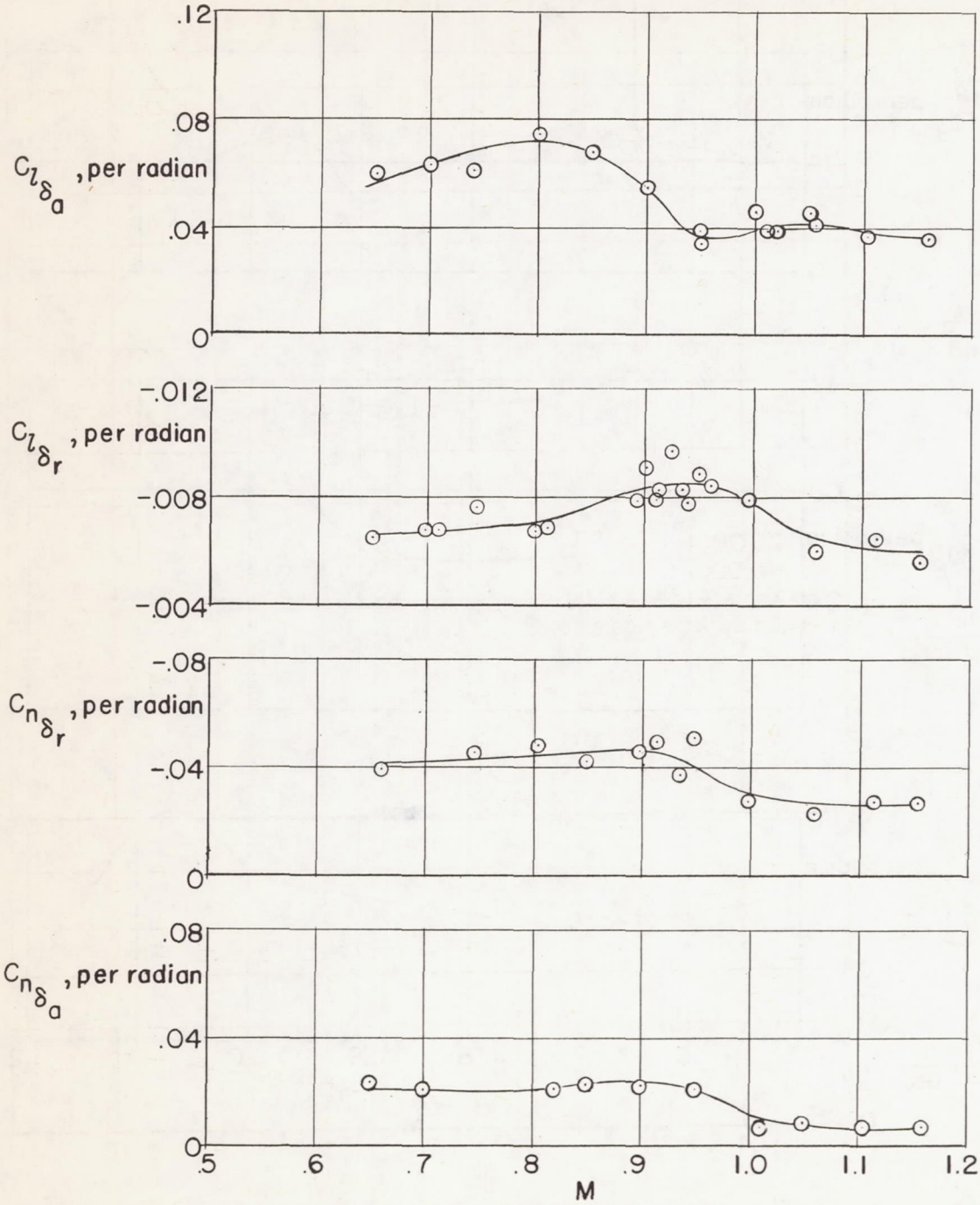

Figure 5.- Stability derivatives determined from flight data at an altitude of 40,000 feet with the Convair YF-102 airplane.

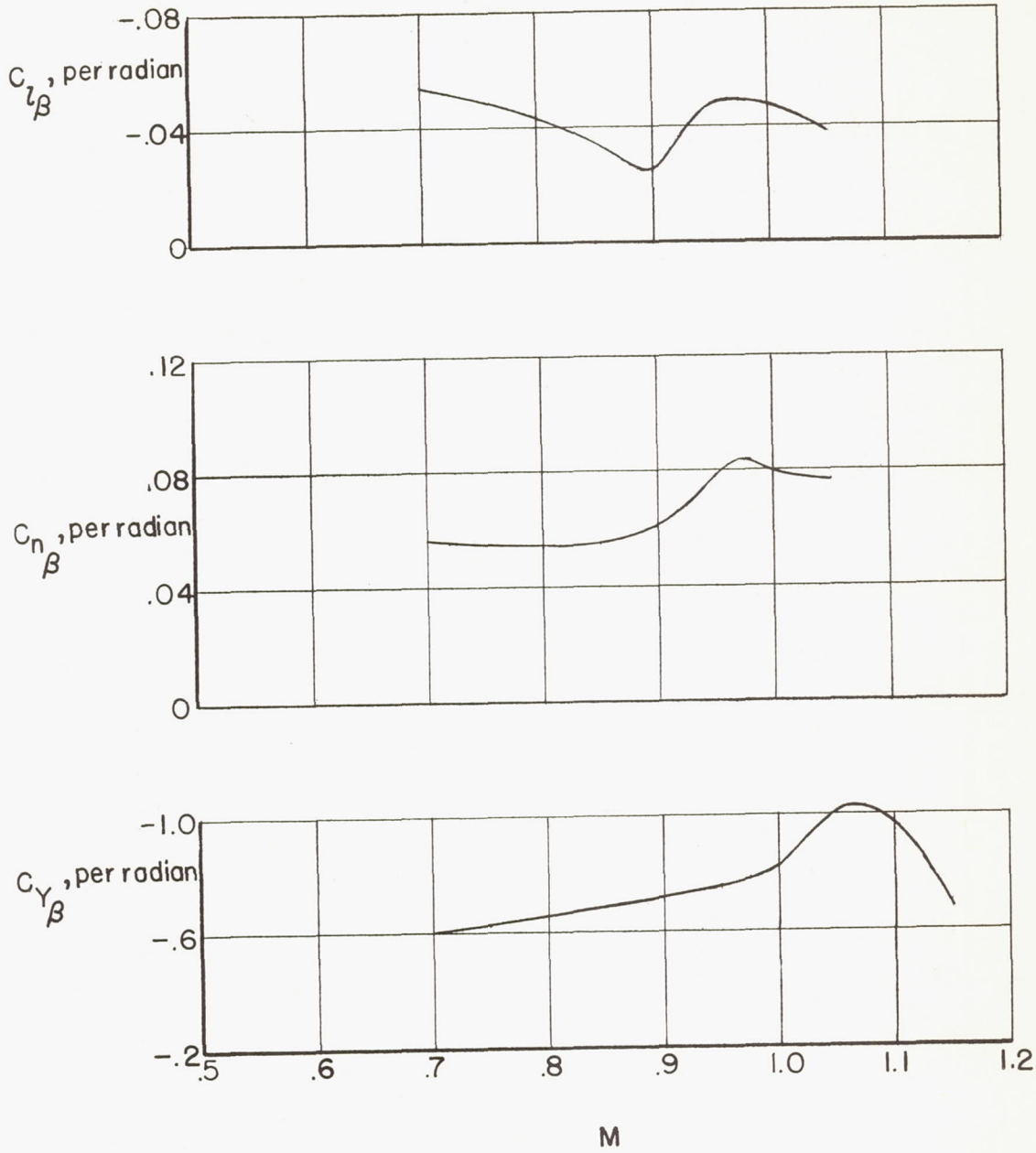

Figure 6.- Calculation of sideslip parameters for the YF-102 airplane. h_p = 40,000 feet.

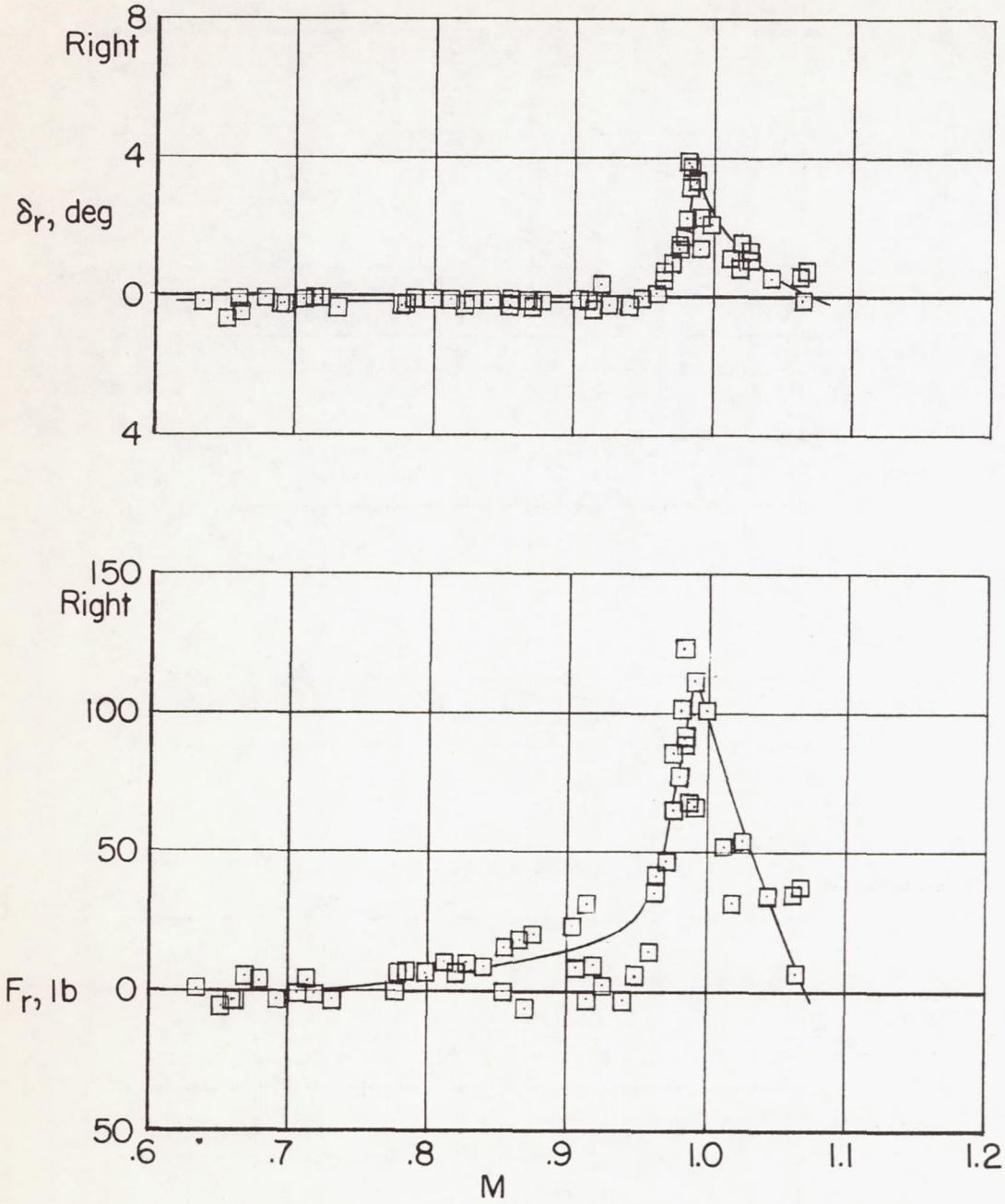

Figure 7.- Rudder required to maintain zero sideslip at h_p = 40,000 feet. YF-102 airplane.

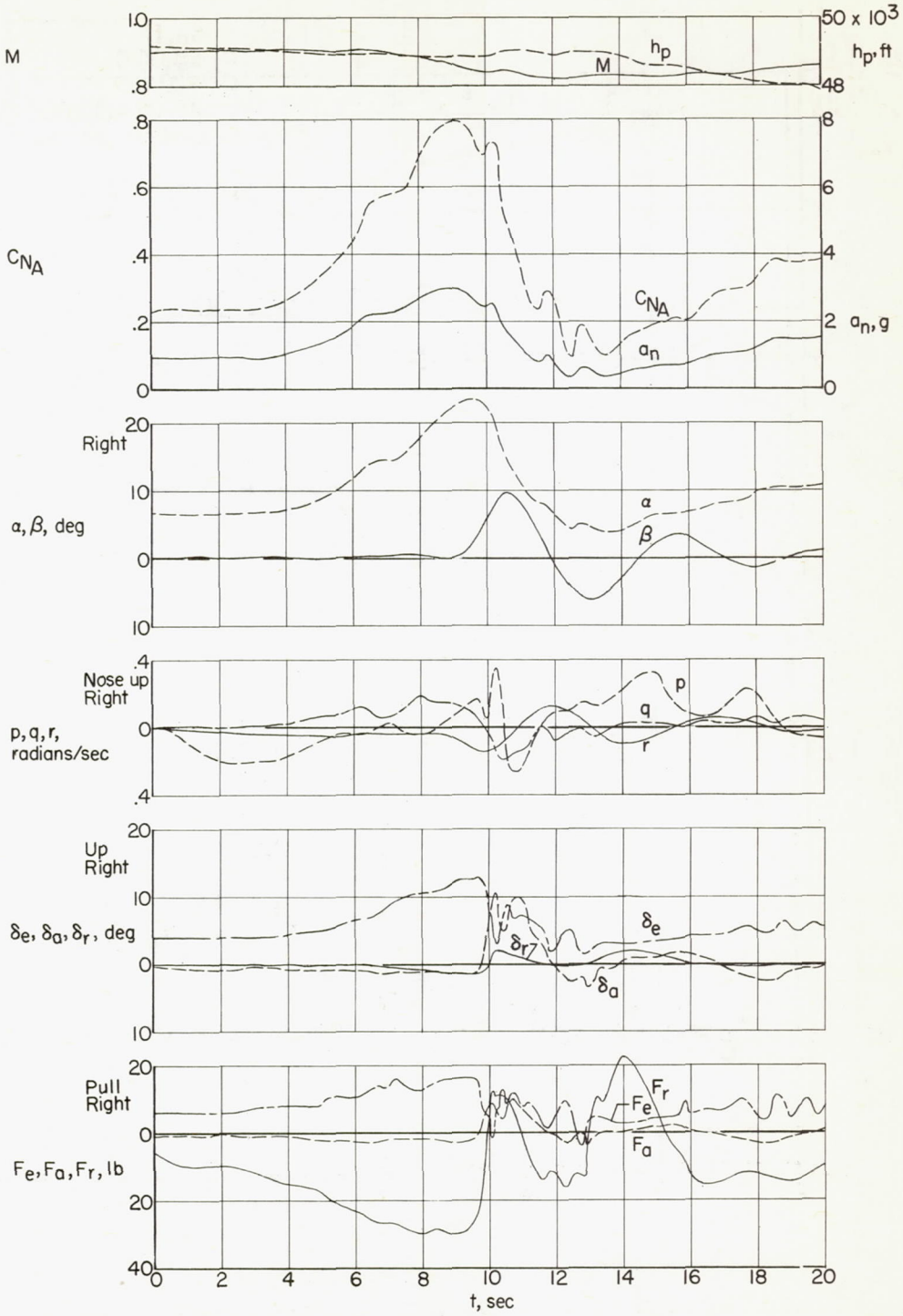

Figure 8.- Wind-up turn at h_p = 50,000 feet in which directional divergence was encountered. YF-102 airplane.

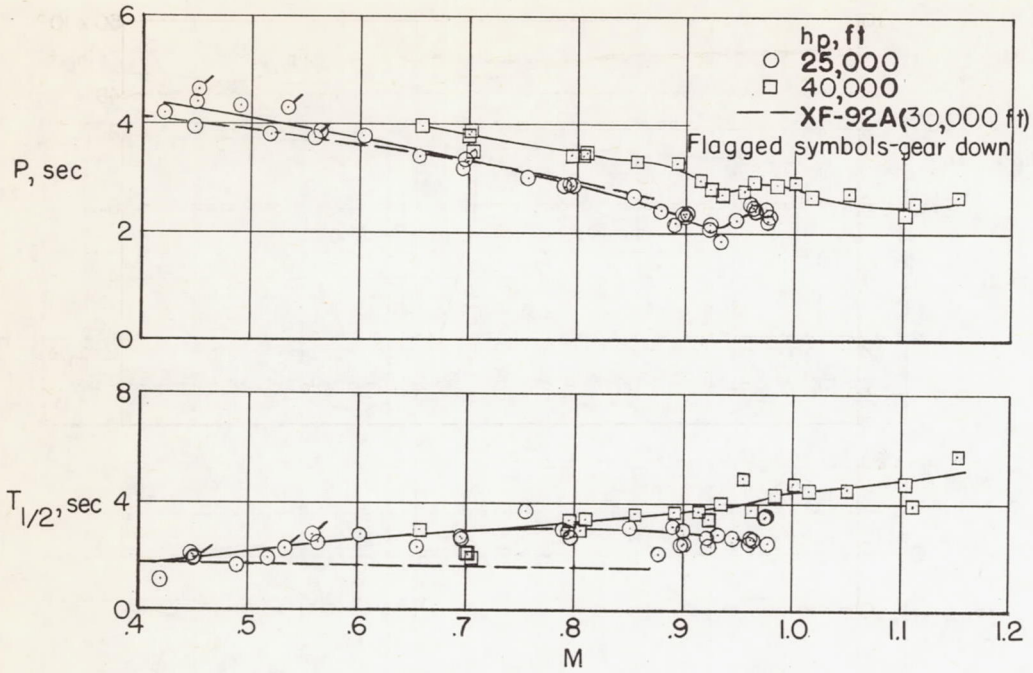

(a) Period and damping.

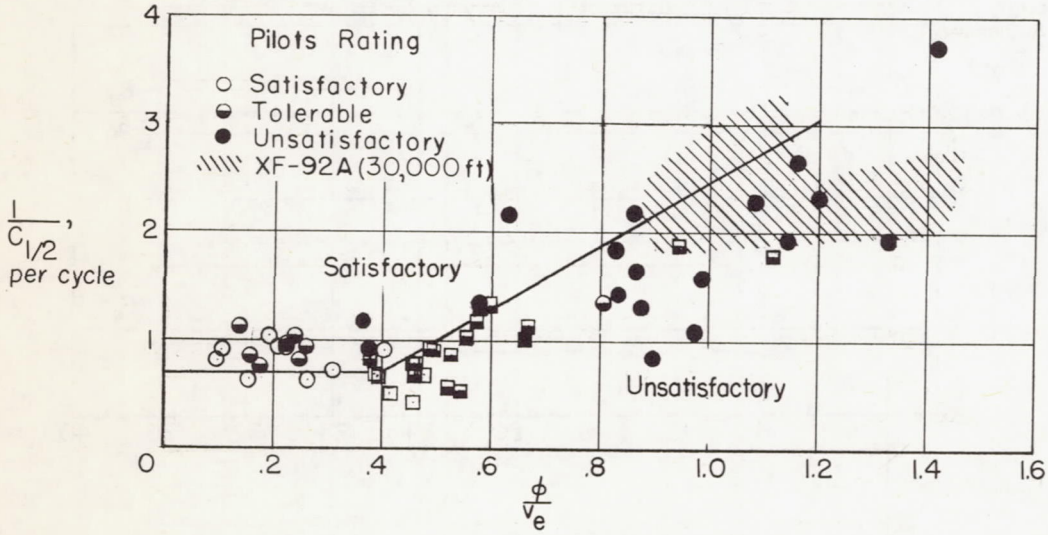

(b) Military specification requirements.

Figure 9.- Period and damping characteristics of the YF-102 airplane obtained from rudder pulses.

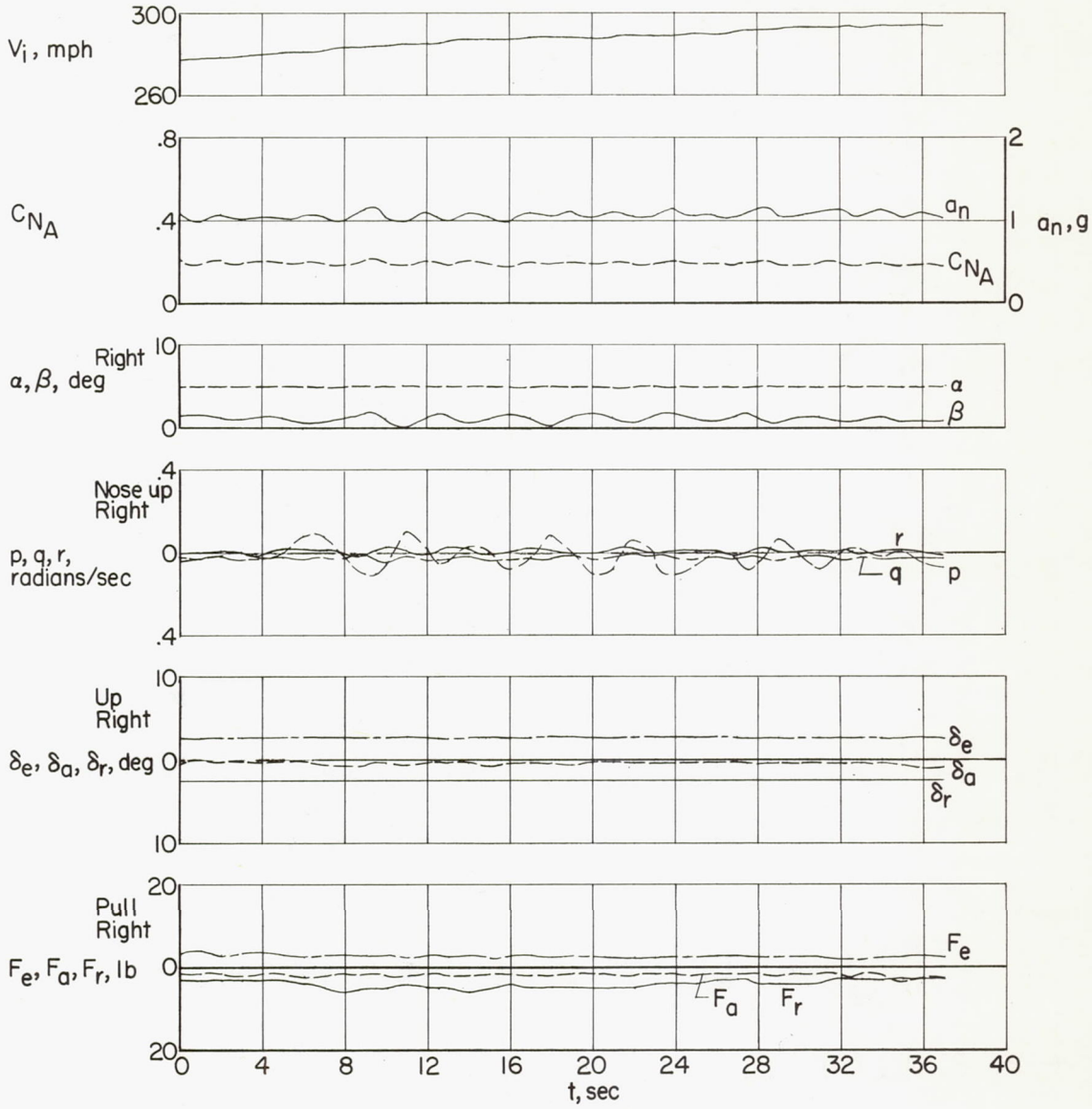

(a) h_p = 21,500 feet.

Figure 10.- Typical residual oscillations encountered on the YF-102 airplane.

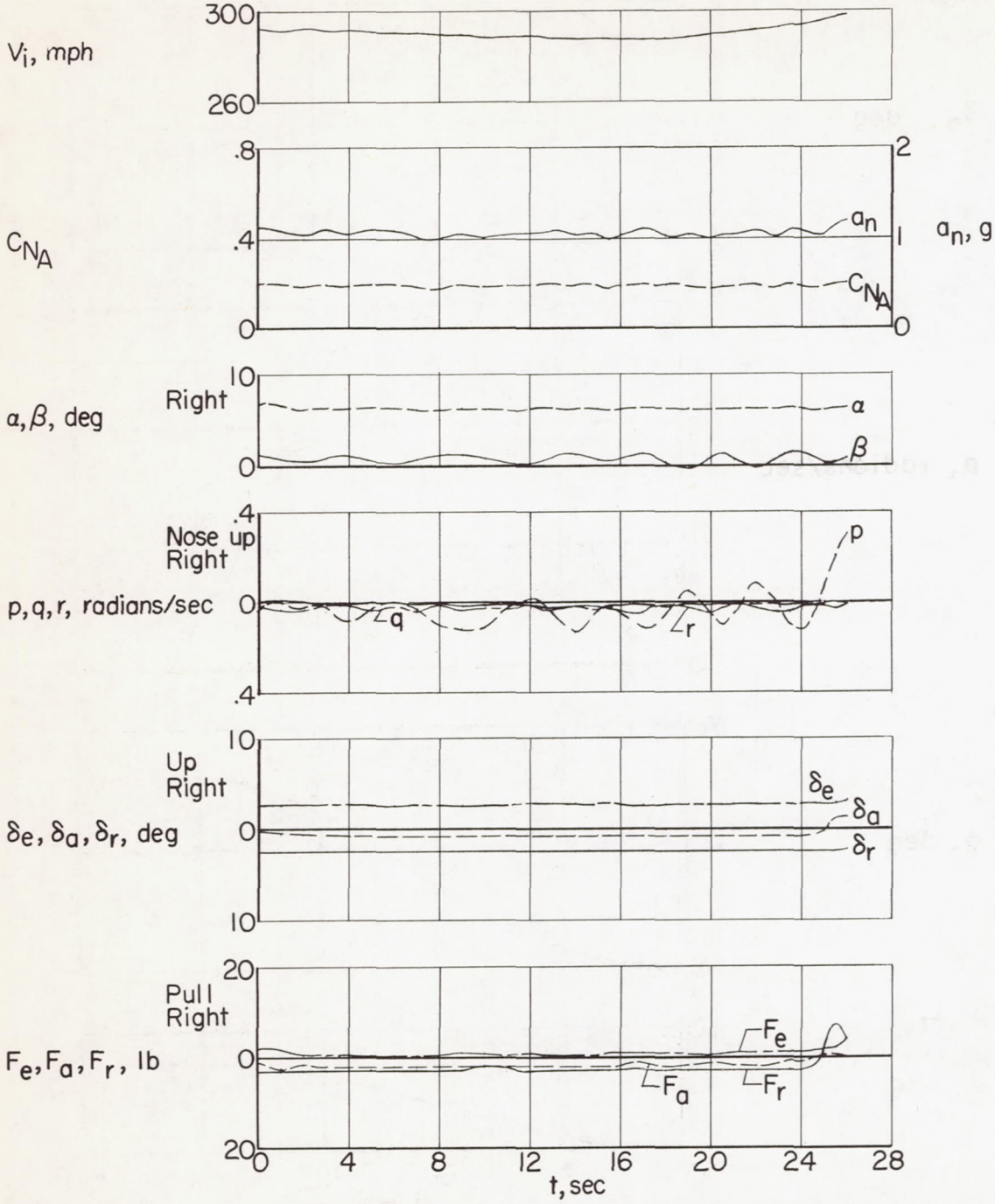

(b) h_p = 22,000 feet.

Figure 10.- Concluded.

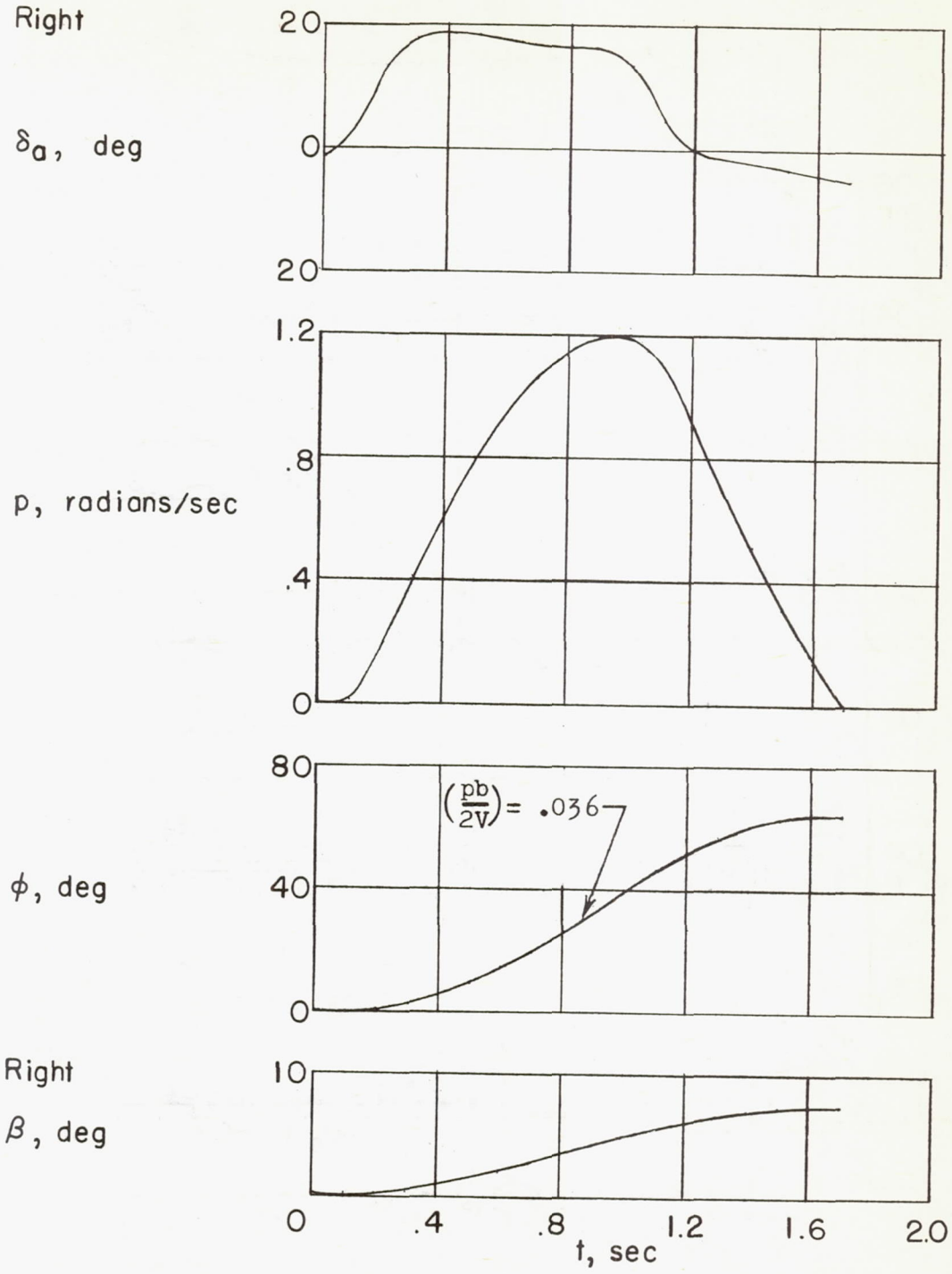

Figure 11.- Time history of a full deflection aileron roll performed at V_i = 150 knots and an altitude of 10,000 feet.

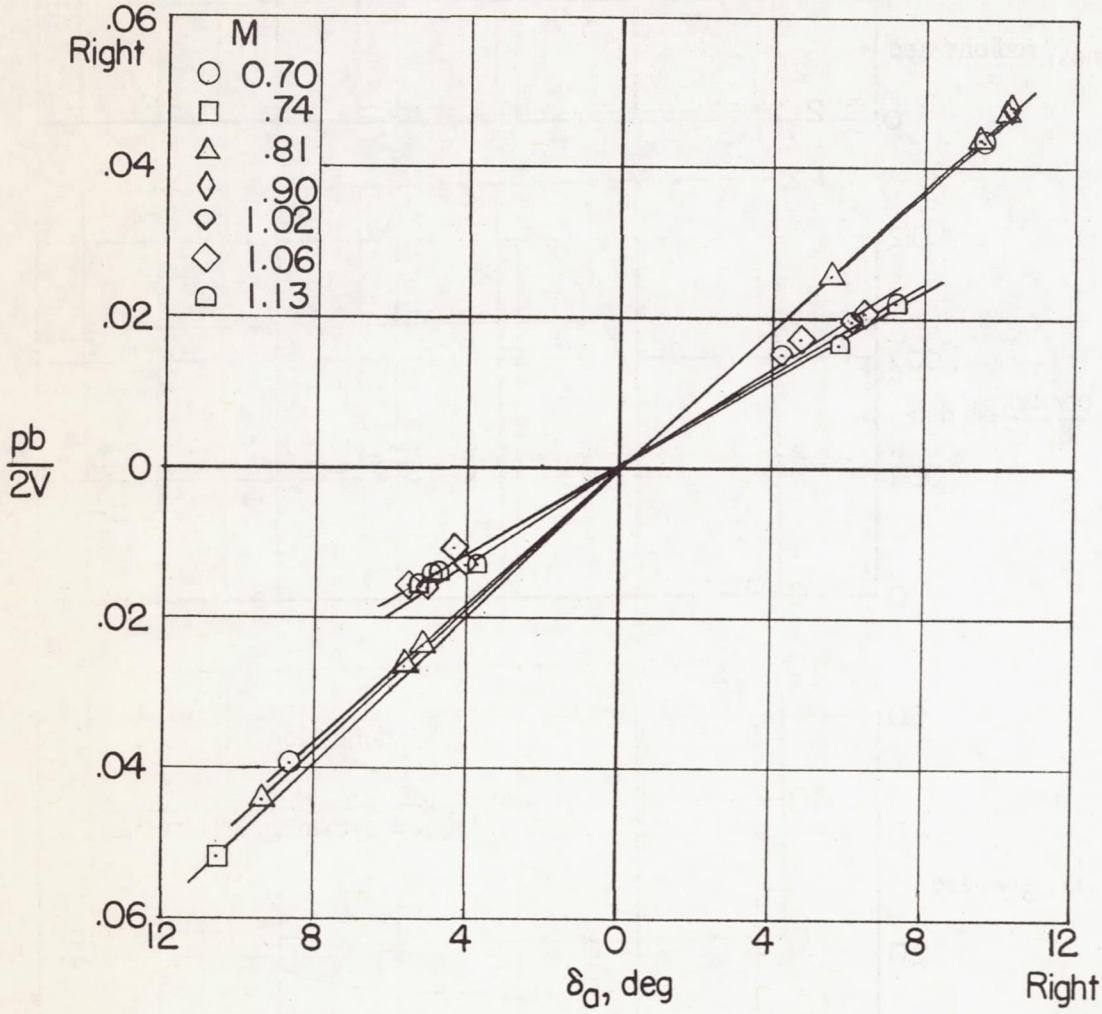

(a) Variation of wing-tip helix angle with lateral control angle.

Figure 12.- Rolling characteristics of the YF-102 airplane.
h_p = 40,000 feet.

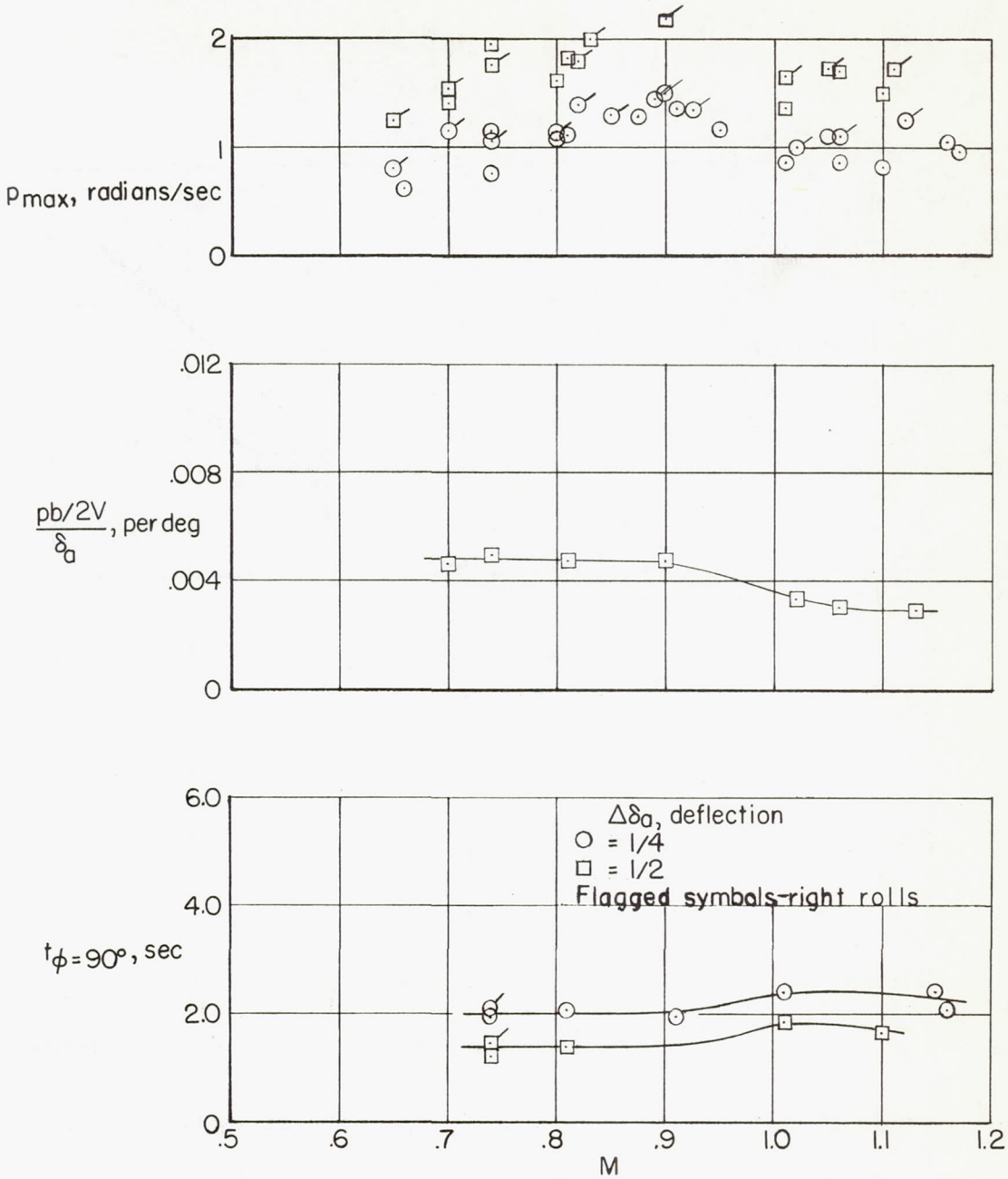

(b) Variation of $\frac{pb/2V}{\delta_a}$ and time to bank to 90° with Mach number.

For the YF-102 airplane. h_p = 40,000 feet.

Figure 12.- Concluded.

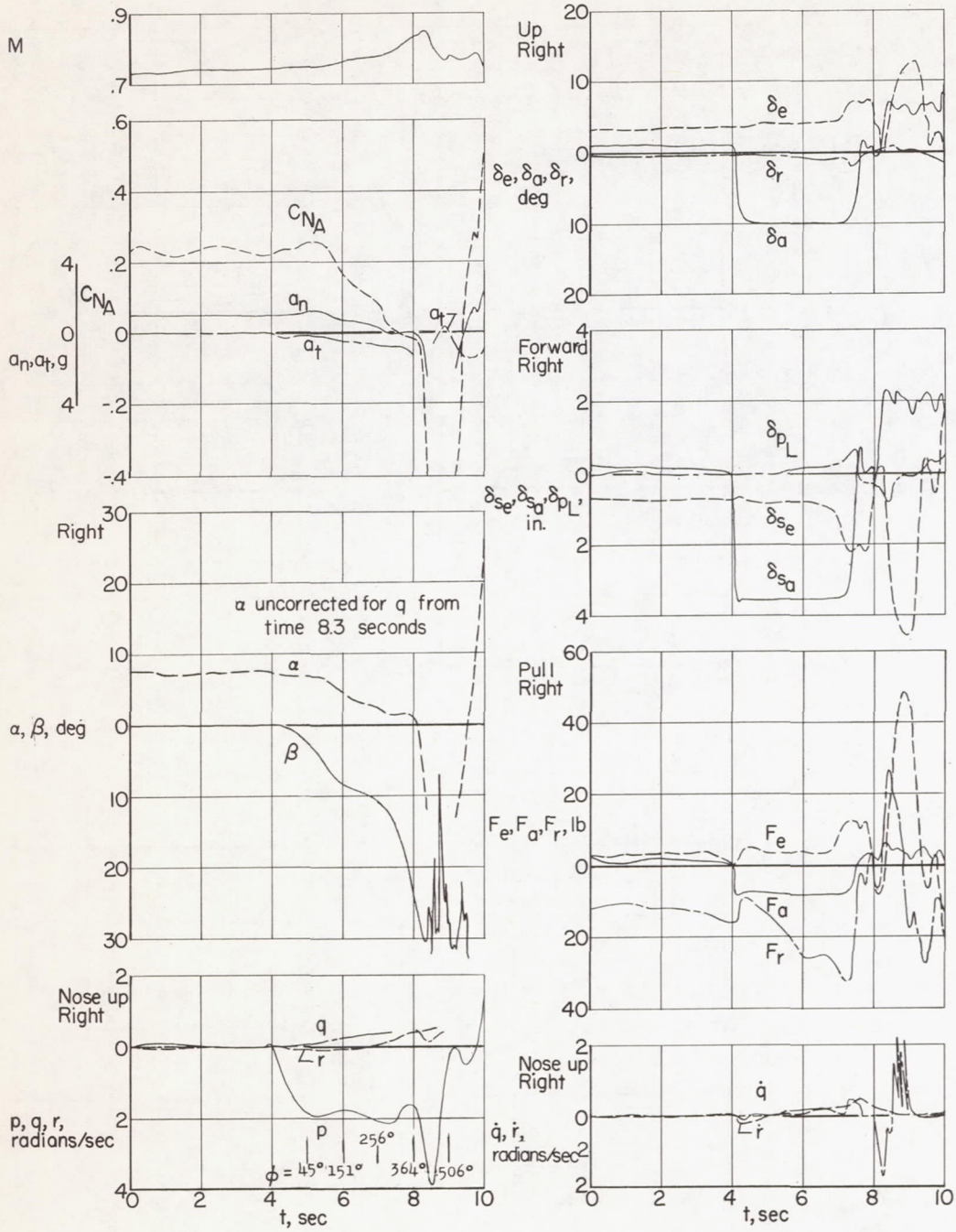

(a) Unrestricted aileron roll in which inertial coupling was experienced.

Figure 13.- Time histories of aileron rolls performed on the YF-102 airplane. h_p = 39,000 feet.

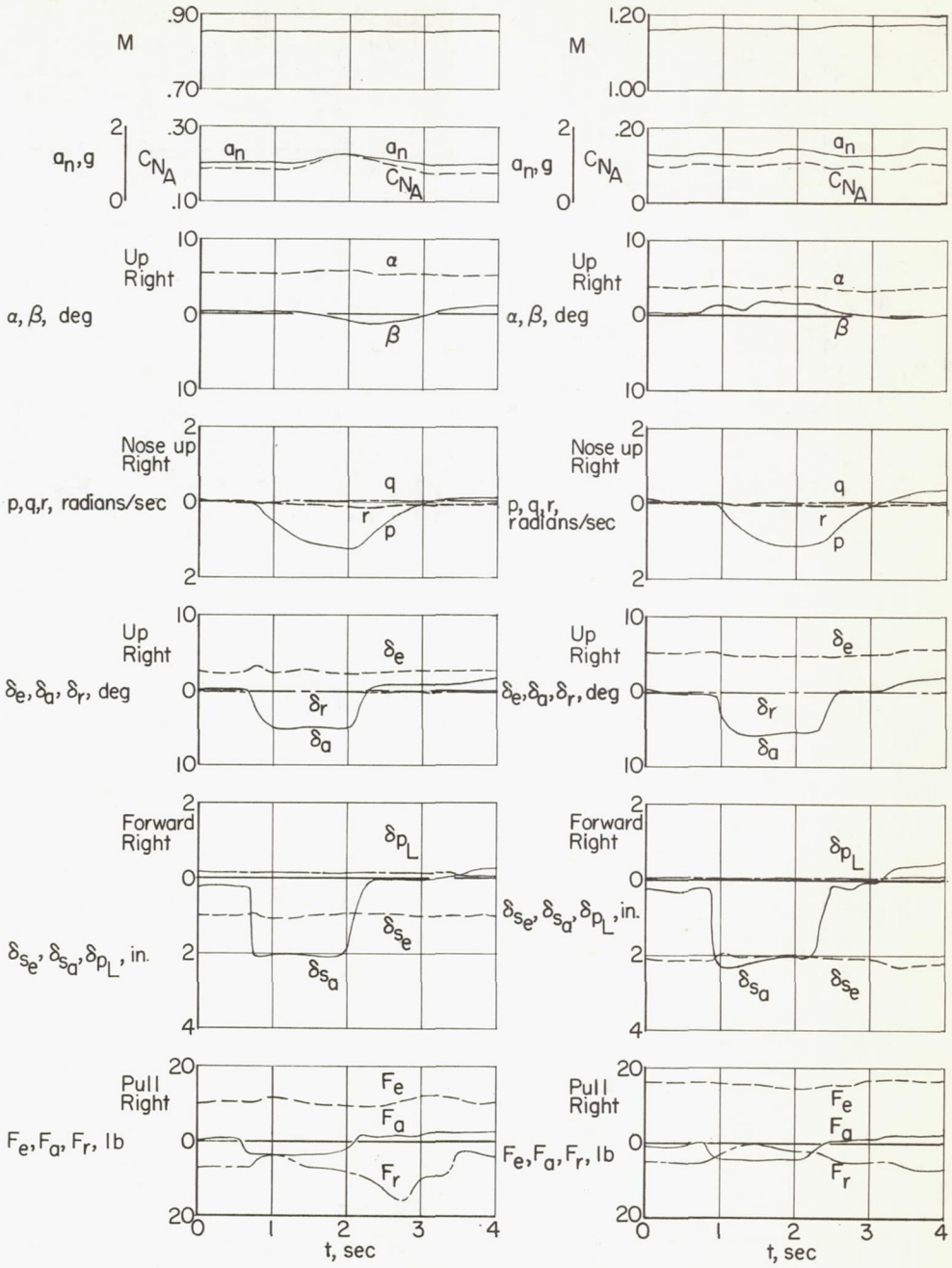

(b) Restricted aileron rolls (100°/sec rate and 100° angle of bank).

Figure 13.- Concluded.

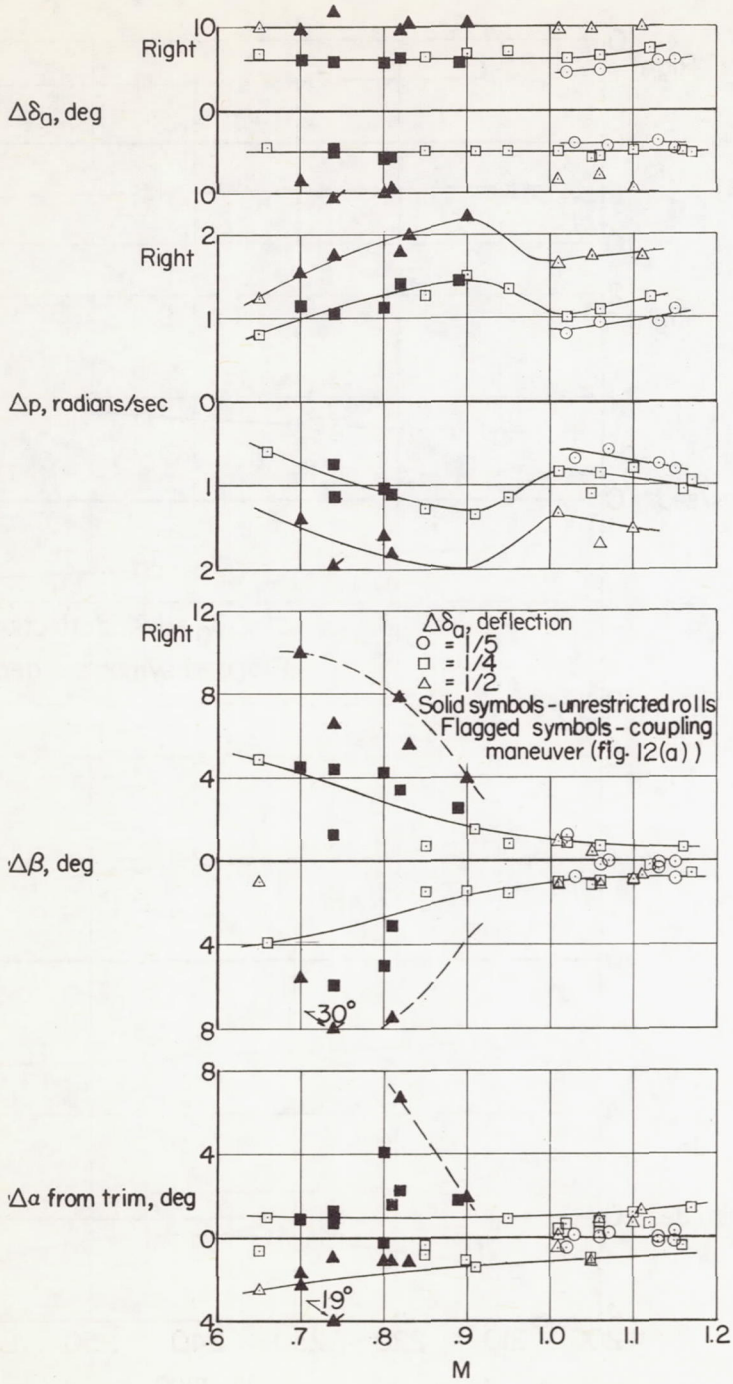

(a) Transonic speed. h_p = 40,000 feet.

Figure 14.- Summary of aileron rolls on the YF-102 airplane.

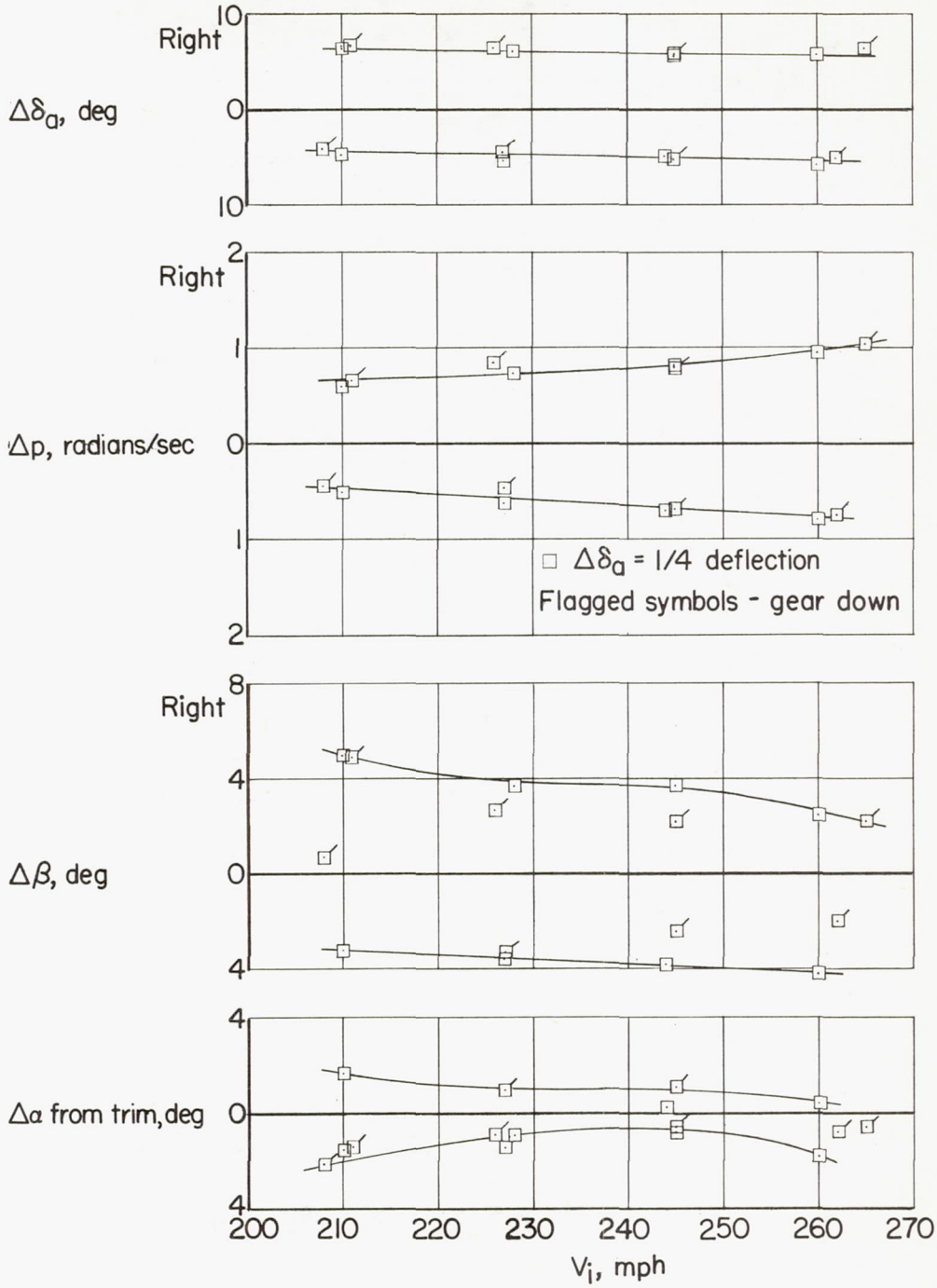

(b) Low speed. h_p = 25,000 feet.

Figure 14.- Concluded.

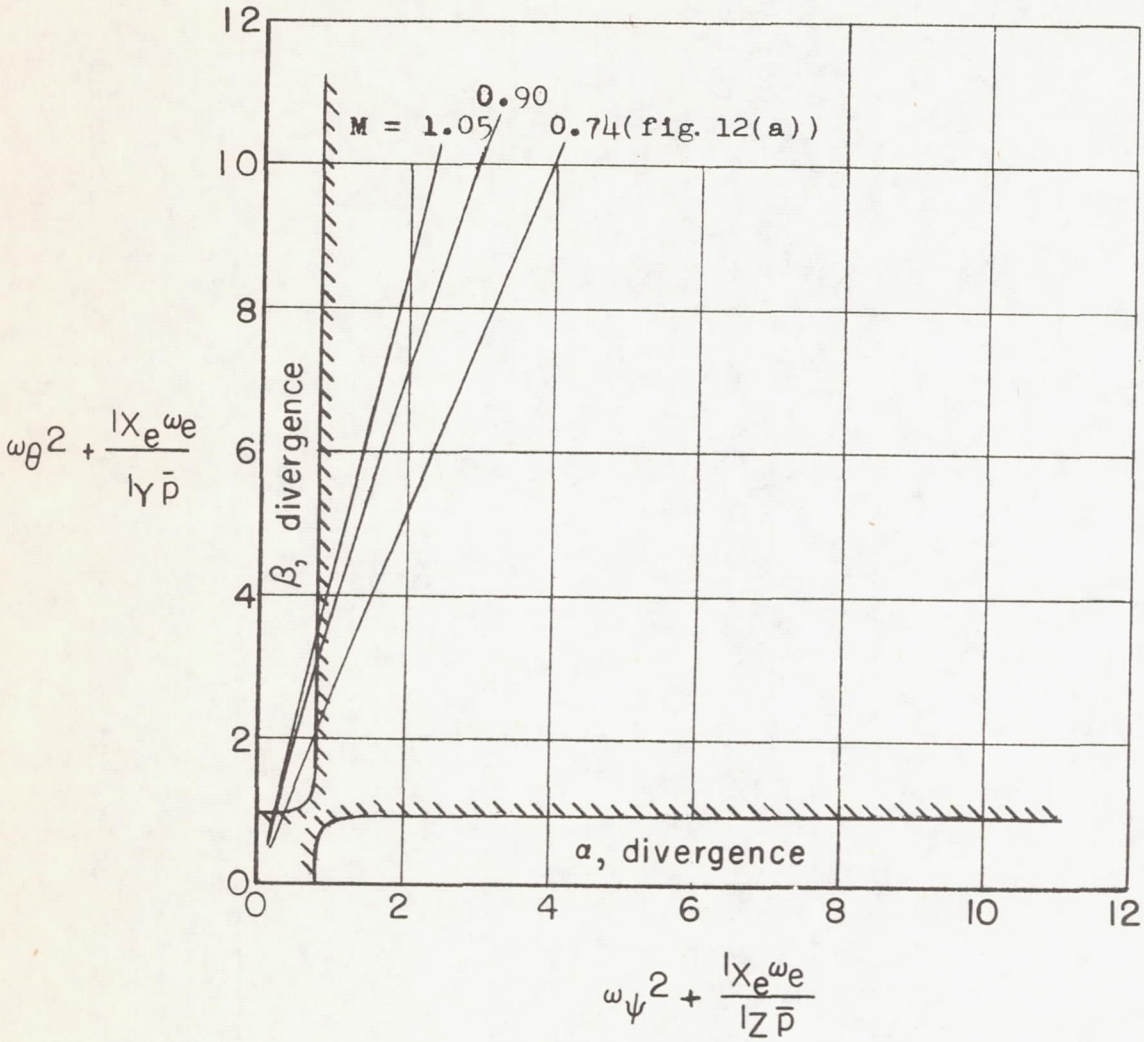

Figure 15.- Stability boundaries for the YF-102 airplane. h_p = 40,000 feet (ref. 4). Left rolls.

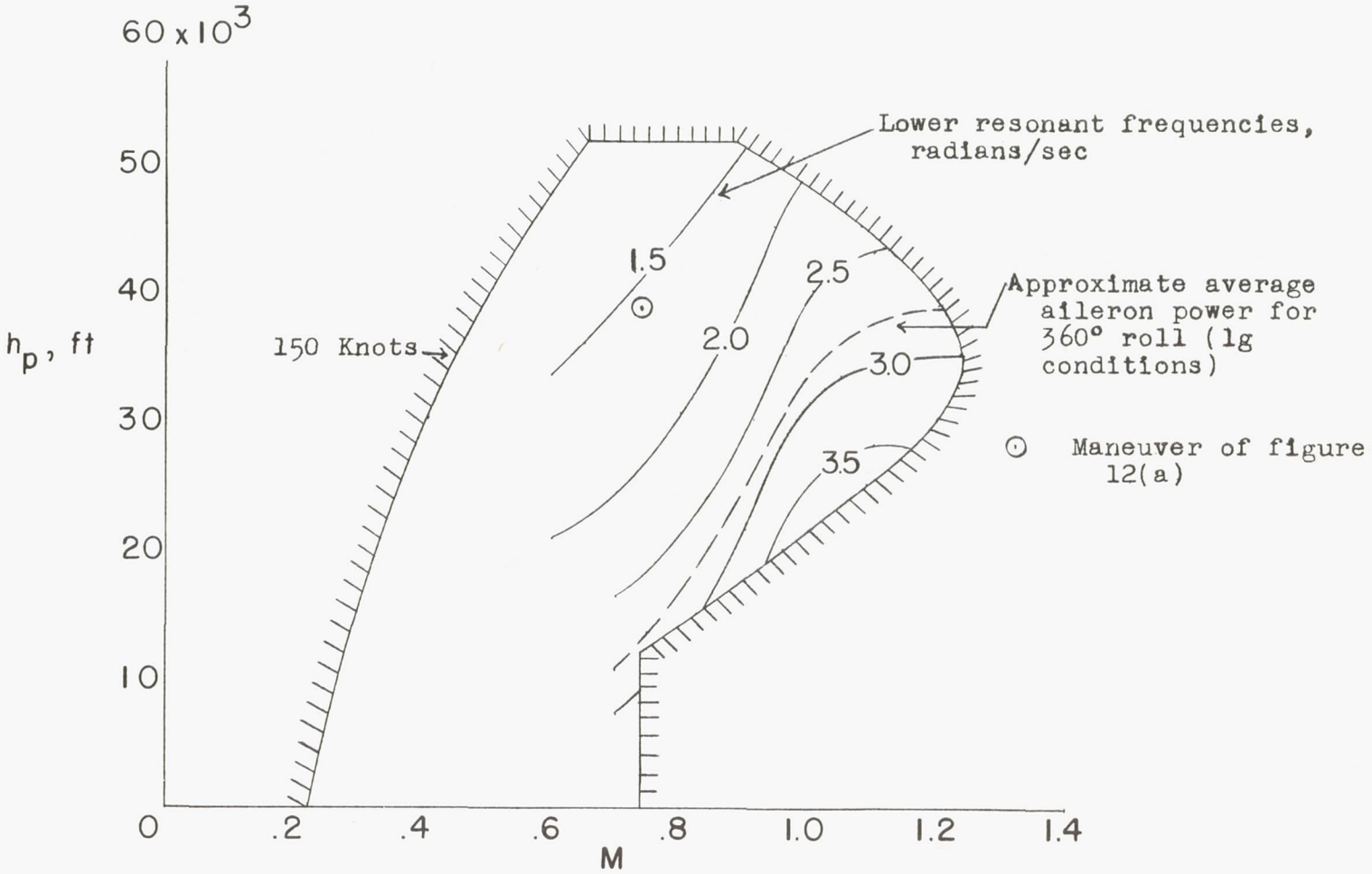

Figure 16.- Guide for predicting inertia coupling of the YF-102 airplane.

NACA - Langley Field, Va.